

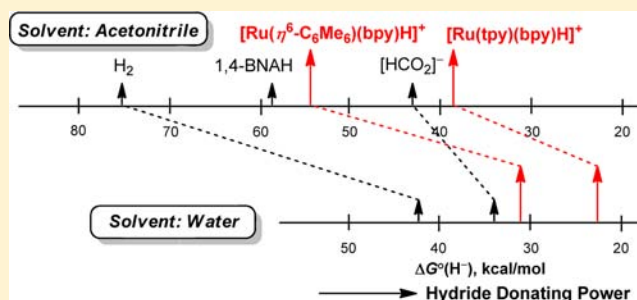
# Thermodynamic and Kinetic Hydricity of Ruthenium(II) Hydride Complexes

Yasuo Matsubara,\* Etsuko Fujita, Mark D. Doherty, James T. Muckerman,\* and Carol Creutz\*

Chemistry Department, Brookhaven National Laboratory, Upton, New York 11973-5000, United States

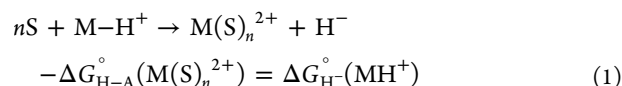
## Supporting Information

**ABSTRACT:** Despite the fundamental importance of the hydricity of a transition metal hydride ( $\Delta G_{\text{H}}^{\circ}(\text{MH})$  for the reaction  $\text{M}-\text{H} \rightarrow \text{M}^+ + \text{H}^-$ ) in a range of reactions important in catalysis and solar energy storage, ours (J. Am. Chem. Soc. 2009, 131, 2794) are the only values reported for water solvent, and there has been no basis for comparison of these with the wider range already determined for acetonitrile solvent, in particular. Accordingly, we have used a variety of approaches to determine hydricity values in acetonitrile of Ru(II) hydride complexes previously studied in water. For  $[\text{Ru}(\eta^6\text{-C}_6\text{Me}_6)(\text{bpy})\text{H}]^+$  (bpy = 2,2'-bipyridine), we used a thermodynamic cycle based on evaluation of the acidity of  $[\text{Ru}(\eta^6\text{-C}_6\text{Me}_6)(\text{bpy})\text{H}]^+$   $\text{p}K_{\text{a}} = 22.5 \pm 0.1$  and the  $[\text{Ru}(\eta^6\text{-C}_6\text{Me}_6)(\text{bpy})(\text{NCCH}_3)_{1/0}]^{2+/0}$  electrochemical potential ( $-1.22$  V vs  $\text{Fc}^+/\text{Fc}$ ). For  $[\text{Ru}(\text{tpy})(\text{bpy})\text{H}]^+$  (tpy = 2,2':6',2''-terpyridine) we utilized organic hydride ion acceptors ( $\text{A}^+$ ) of characterized hydricity derived from imidazolium cations and pyridinium cations, and determined  $K$  for the hydride transfer reaction,  $\text{S} + \text{MH}^+ + \text{A}^+ \rightarrow \text{M}(\text{S})^{2+} + \text{AH}$  ( $\text{S} = \text{CD}_3\text{CN}$ ,  $\text{MH}^+ = [\text{Ru}(\text{tpy})(\text{bpy})\text{H}]^+$ ), by  $^1\text{H}$  NMR measurements. Equilibration of initially 7 mM solutions was slow—on the time scale of a day or more. When  $E^{\circ}(\text{H}^+/\text{H}^-)$  is taken as 79.6 kcal/mol vs  $\text{Fc}^+/\text{Fc}$  as a reference, the hydricities of  $[\text{Ru}(\eta^6\text{-C}_6\text{Me}_6)(\text{bpy})\text{H}]^+$  and  $[\text{Ru}(\text{tpy})(\text{bpy})\text{H}]^+$  were estimated as  $54 \pm 2$  and  $39 \pm 3$  kcal/mol, respectively, in acetonitrile to be compared with the values 31 and 22 kcal/mol, respectively, found for aqueous media. The  $\text{p}K_{\text{a}}$  estimated for  $[\text{Ru}(\text{tpy})(\text{bpy})\text{H}]^+$  in acetonitrile is  $32 \pm 3$ . UV-vis spectroscopic studies of  $[\text{Ru}(\eta^6\text{-C}_6\text{Me}_6)(\text{bpy})]^0$  and  $[\text{Ru}(\text{tpy})(\text{bpy})]^0$  indicate that they contain reduced bpy and tpy ligands, respectively. These conclusions are supported by DFT electronic structure results. Comparison of the hydricity values for acetonitrile and water reveals a flattening or compression of the hydricity range upon transferring the hydride complexes to water.



## INTRODUCTION

The ability of a molecule  $\text{A}-\text{H}$  to serve as a hydride ion donor has been denoted as its hydride affinity<sup>1,2</sup> [ $\Delta G_{\text{H}-\text{A}}^{\circ}(\text{A}^+)$ ] or hydricity<sup>3</sup> [ $\Delta G_{\text{H}}^{\circ}(\text{AH})$ ]:  $\text{A}-\text{H} \rightarrow \text{A}^+ + \text{H}^-$ ,  $-(\Delta G_{\text{H}-\text{A}}^{\circ}(\text{A}^+)) = \Delta G_{\text{H}}^{\circ}(\text{AH})$ . The hydricity of a transition-metal hydride complex  $\text{MH}$ , defined here<sup>4</sup> in eq 1 ( $\text{S}$  is a solvent molecule,  $n = 1$  or 0),



is important in a number of catalytic sequences,<sup>5-7</sup> including processes central to solar energy conversion.<sup>8</sup> We recently used the reaction of carbon dioxide with two Ru(II) hydride complexes to estimate their hydricities in water.<sup>9,10</sup> Since few other data are available for water, and because such thermodynamic measurements are often made in acetonitrile, we have now examined the hydricity thermodynamics of these Ru(II) hydride complexes in acetonitrile. The only other Ru(II) complex to be similarly characterized is  $\text{CpRu}(\text{CO})_2\text{H}$ .<sup>11</sup>

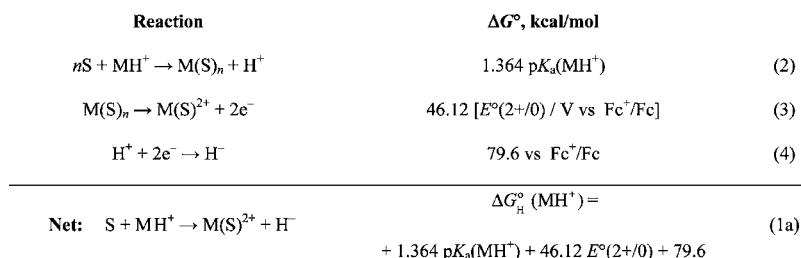
Hydricity measurements are experimentally challenging. DuBois has pioneered the determination of transition-metal hydricity, largely by deploying thermodynamic cycles such as that in Scheme 1,<sup>12</sup> in turn inspired by analogous studies<sup>13</sup> of purely

organic systems and studies of bond dissociation energies. Scheme 1 develops the analogy between acidity (eq 2) and hydricity (eq 1). The hydricity is obtained from measurements of eqs 2 and 3 and use of eq 1a (Scheme 1). The free-energy change of 79.6 kcal/mol for eq 4<sup>12</sup> at 298.15 K is obtained from two terms: (1) the reduction potentials given by Wayner and Parker<sup>13</sup> for the  $\text{H}^+/\text{H}^{\bullet}$  ( $-1.77$  V vs NHE) and  $\text{H}^{\bullet}/\text{H}^-$  ( $-0.60$  V vs NHE) couples, which are converted to  $-2.30$  and  $-1.13$  V vs  $\text{Fc}^+/\text{Fc}$ , respectively, by using a potential for the  $\text{Fc}^+/\text{Fc}$  couple ( $+0.528$  V vs NHE)<sup>14,15</sup> in acetonitrile solution, and (2) the small modification ( $+0.6$  kcal/mol)<sup>16</sup> for the  $\text{H}^+/\text{H}^{\bullet}$  couple suggested by DuBois.

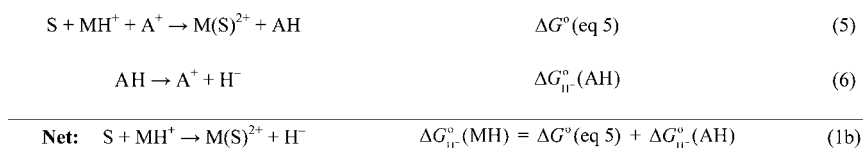
In most systems considered previously,<sup>3</sup> no solvent addition accompanies hydride or proton loss, i.e.,  $n = 0$  for all processes. In the systems to be considered here, the chemistry is more complicated in that a solvent molecule binds to the metal upon hydride ion loss ( $n = 1$ ) and may (discussed later) also bind the reduced species. The detailed consequences of solvent acetonitrile binding to the several relevant metal oxidation states have recently been reported by Roberts et al.,<sup>17,18</sup> who found the

Received: March 26, 2012

Published: September 11, 2012

Scheme 1. Cycle 1 for Evaluation of Hydricity in CH<sub>3</sub>CN

## Scheme 2. Cycle 2 for Evaluation of Hydricity



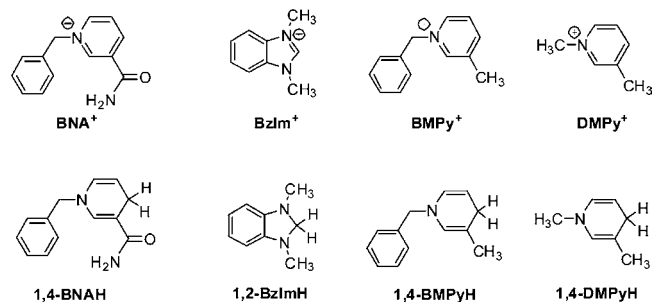
dissociation constant for acetonitrile from W(II) to be  $10^{-13}$  M. On the other hand, as noted by Wilson et al.,<sup>19</sup> since the activity of the solvent is conventionally taken as unity, the net free-energy changes for Scheme 1 remain valid as long as the solvent S is not changed. Whenever two different solvents are compared, the relative stabilities of, for example, aqua and acetonitrile complexes affect the heterolysis thermodynamics. Finally, solvent may influence redox thermodynamics even when it is not directly bonded to the metal center. Large effects have been found for entirely outer-sphere solvent when specific solute–solvent interactions are possible.<sup>20</sup> For the present case the aromatic ligands are expected to be largely indifferent to solvent, but the hydride ligand is expected to engage in dihydrogen bonding<sup>21</sup> with hydrogen-bond-donating solvents. Furthermore, the ligand, rather than the metal, may serve as the reduction site. These complications are addressed as needed in later sections of the paper.

Utilization of Scheme 1 involves deprotonation of the hydride complex, typically by an N-centered Brønsted base, and, in a separate measurement, determination of the two-electron reduction potential of  $M(S)^{2+}$ . Norton has demonstrated that the barriers to proton transfer between transition-metal and N- or O-centered bases, while greater than those between N- or O-centered acids and bases, are moderate.<sup>22–26</sup> Thus eq 2 is expected to be experimentally realizable, and this has proven the case. Relative values of acidities (eq 2) have also been obtained by Angelici and colleagues, who measured enthalpies of protonation of a number of neutral complexes in dichloromethane.<sup>27</sup> Similarly, electrochemical evaluation of eq 3 is, in principle, straightforward.

An alternative thermodynamic cycle for the determination of hydricity involves equilibration (eq 5) of a transition-metal hydride with a hydride acceptor  $A^+/AH$  (usually an organic molecule) of known hydricity (eq 6) to give the hydride donor ability (eq 1b) (Scheme 2).

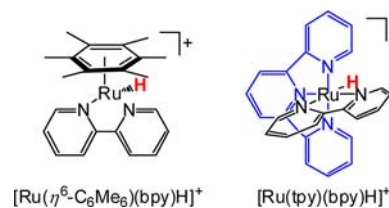
Zhu et al. have recently developed a broad database of electrochemical and thermochemical data bearing on hydricity thermodynamics.<sup>28–32</sup> Although those enthalpy values they have reported are incorrect systematically by  $-32.8$  kcal/mol as discussed later, these organic acceptors potentially provide a broad flexible tool for investigation of transition-metal systems. Acceptors to be discussed or used in the present study are depicted in Chart 1 along with their abbreviations. The Ru(II)

## Chart 1. Organic Hydride Acceptors and Their Conjugate Donors



hydrides used are shown in Chart 2. Note that in the present study (unlike most others) hydride acceptors of hydricity

## Chart 2. Ru(II) Hydride Donors



comparable to those of the Ru–H complex have been selected in an effort to measure the rate constants at low driving force for eq 5.

Sarker and Bruno sought to use equilibration with trityl cation derivatives in acetonitrile solvent<sup>33</sup> but, misled by apparent equilibrium, determined values that greatly underestimated hydride donor abilities (overestimated  $\Delta G_{\text{H}}^\circ$ ) for the systems studied.<sup>16</sup> Berning and DuBois attempted equilibration of diphosphine hydride complexes with BNA<sup>+</sup> but found the reactions to be too slow to be useful.<sup>12</sup> Indeed, these early papers point to a general problem in this field—the slowness of equilibration of many hydride-transfer equilibria. The purely organic reactions of dihydropyridines with acridinium ion are so intrinsically slow as to be accessible by stopped-flow methods despite their enormous exothermicity: for example,  $\Delta H < -32$  kcal/mol and the second-order rate constant at 298 K is only ca.  $10^2 \text{ M}^{-1} \text{ s}^{-1}$  ( $\Delta G^\ddagger = 14.9$  kcal/mol) for 1,4-BNAH as hydride

Table 1. Redox Potentials of Ru(II) Complexes<sup>a</sup> at 298 ± 5 K

| complex   | $E_{1/2}/V$ vs $Fc^+/Fc$ in acetonitrile ( $\Delta E_p/mV$ )             |
|---|--|
| $[Ru(\eta^6-C_6Me_6)(bpy)(NCCH_3)]^{2+}$            | -1.22 (59)   |
| $[Ru(\eta^6-C_6Me_6)(bpy)(OH_2)]^{2+}$ <sup>b</sup> | ≤ -1.21 <sup>c,d</sup>   |
| $[Ru(\eta^6-C_6Me_6)(bpy)H]^+$ <sup>e</sup>         | +0.32 <sup>c</sup>   |
| $[Ru(tpy)(bpy)(NCCH_3)]^{2+}$ <sup>f</sup>          | +0.91 (75), -1.68 (88), -1.98 (92), -2.33 (96)                           |
| $[Ru(tpy)(bpy)(OH_2)]^{2+}$ <sup>b,g</sup>          | ≤ -1.83 <sup>c,h</sup> ≤ -2.02 <sup>c,i</sup>                            |
| $[Ru(tpy)(bpy)H]^+$ <sup>j,k</sup>                  | +0.16 (156) <sup>l</sup> -1.98 (66) <sup>m</sup> -2.23 (70) <sup>m</sup> |

<sup>a</sup>Half-wave potentials determined by CV (scan rate 0.1 V/s), otherwise peak potential determined by OSWV (staircase step height, SW amplitude and frequency are 4 mV, 25 mV and 15 Hz) in acetonitrile solution containing the complex (1 mM) and TBAH (0.1 M) under an Ar atmosphere, except as noted. A glassy carbon was used as a working electrode. <sup>b</sup>In sodium phosphate buffer ( $\mu = 0.1$  M, pH = 6.8). <sup>c</sup>Peak potential. <sup>d</sup>Converted value from -0.77 V vs Ag/AgCl by addition of +0.045 V (i.e., conversion to SCE scale), +0.250 V<sup>14</sup> (i.e., conversion from SCE to NHE scale), and then -0.528 V<sup>15</sup> (i.e., conversion from NHE scale to  $Fc^+/Fc$  scale). Only the cathodic portion was observed (Figure 1b). <sup>e</sup>Frequency 60 Hz. <sup>f</sup>Scan rate 0.8 V/s. <sup>g</sup>A Hg drop was used as a working electrode. <sup>h</sup>Converted value from -1.39 V vs Ag/AgCl by the method in the footnote *d* above. <sup>i</sup>Converted value from -1.58 V vs Ag/AgCl by the method in the footnote *d* above. <sup>j</sup>A carbon fiber microelectrode was used as working electrode. <sup>k</sup>Concentrations of 5 mM of the complex and 0.6 M of TBAH. <sup>l</sup>Scan rate 10 kV/s. <sup>m</sup>Scan rate 25 V/s.

donor with acridinium ion acceptor.<sup>30</sup> For reaction of a metal hydride with an organic hydride acceptor, a similar conclusion may be drawn, although fewer data are available. Despite Bullock's broad studies of relative kinetic hydricity of transition-metal hydrides involving trityl cation acceptors,<sup>34,35</sup> one of the few (only?) examples of known hydricity change appears to be that of a trityl cation with a Mo(II)-hydride: Ellis et al. reported hydricity values for  $CpMo(CO)_2(PMe_3)H$  and  $Cp^*Mo(CO)_2(PMe_3)H$  of 55 and 58 kcal/mol, respectively, in acetonitrile.<sup>16</sup> Bullock<sup>34</sup> determined rate constants for the reaction of  $CpMo(CO)_2(PMe_3)H$  with trityl cation ( $\Delta G_{H^-}^\circ = 99$  kcal/mol in acetonitrile) in dichloromethane to be  $4.6 \times 10^6$   $M^{-1} s^{-1}$  at 298 K ( $\Delta G^\ddagger = 8.4$  kcal/mol), and Bruno<sup>33</sup> determined that of  $7.5 \times 10^3$   $M^{-1} s^{-1}$  for (*p*-MeOPh)<sub>2</sub>PhC<sup>+</sup> ( $\Delta G_{H^-}^\circ = 89.3$  kcal/mol) in acetonitrile. Thus, it is anticipated that equilibration between transition-metal hydrides and organic acceptors may be rather slow at small driving force.

In this account we report electrochemical, UV-vis spectroscopic, and NMR studies bearing on the properties, reaction thermodynamics, and kinetics of  $[Ru(\eta^6-C_6Me_6)(bpy)H]^+$  (bpy = 2,2'-bipyridine) and  $[Ru(tpy)(bpy)H]^+$  (tpy = 2,2':6',2''-terpyridine) and their conjugate bases in acetonitrile. We also use DFT calculations to probe the coordination numbers and geometries of the reduced ruthenium complexes.

## EXPERIMENTAL SECTION

**Materials.** Acetonitrile (Aldrich, Chromasolv Plus grade) was dried over activated 3A molecular sieves and vacuum-transferred prior to use. Acetonitrile-*d*<sub>3</sub> was purified by refluxing over alkaline  $KMnO_4$ , distilling, drying over  $CaH_2$ , and then vacuum-transferring before use. 1,1,3,3-Tetramethylguanidine (TMG) was distilled from KOH and used immediately. *n*-Bu<sub>4</sub>NPF<sub>6</sub> (TBAH) was recrystallized in the published manner.<sup>36</sup> Other purchased chemicals were ACS reagent grade and used without purification. The compounds  $[Ru(\eta^6-C_6Me_6)(bpy)H](PF_6)$ ,<sup>37</sup>  $[Ru(\eta^6-C_6Me_6)(bpy)H](OTf)$  (OTf = trifluoromethanesulfonate),<sup>9</sup>  $[Ru(tpy)(bpy)(NCCH_3)](PF_6)$ ,<sup>38</sup>  $W(CO)_5(NCCH_3)$ ,<sup>39,40</sup> [Pt-(depe)<sub>2</sub>](PF<sub>6</sub>)<sub>2</sub> (depe = 1,2-bis(diethylphosphino)ethane),<sup>41</sup> [Pt-(dppe)<sub>2</sub>](PF<sub>6</sub>)<sub>2</sub> (dppe = 1,2-bis(diphenylphosphino)ethane),<sup>42</sup> and the hexafluorophosphate salts of hydride acceptors (BzIm<sup>+</sup>,<sup>28</sup> BMpy<sup>+</sup>,<sup>30</sup> and DMpy<sup>+</sup><sup>43</sup>) were prepared according to the reported methods.

**Synthesis of  $[Ru(\eta^6-C_6Me_6)(NCCH_3)](PF_6)_2$ .** Five milliliters of water containing  $[Ru(\eta^6-C_6Me_6)Cl_2]_2$  (25 mg, 0.037 mmol)<sup>44</sup> and  $Ag_2SO_4$  (24 mg, 0.077 mmol) was sonicated intermittently for 1 h during which the brown solid dissolved to afford a yellow solution. The precipitated white solid (AgCl) was removed by filtration. To the filtrate was added 2,2'-bipyridine (12 mg, 0.077 mmol). The solution was stirred for 12 h and excess  $NH_4PF_6$  was added to precipitate the complex. The orange solid was dissolved in 2 mL of acetonitrile, and

then 10 mL of ether was added to produce a yellow crystalline solid. Yield: 30 mg, 53%. <sup>1</sup>H NMR ( $\delta$ , acetonitrile-*d*<sub>3</sub>): 8.87 (2H, ddd, *J* = 5.7, 1.4, 0.7 Hz, bpy-6), 8.36 (2H, d, *J* = 8.1 Hz, bpy-3), 8.26 (2H, ddd, *J* = 8.1, 7.6, 1.4 Hz, bpy-4), 7.83 (2H, ddd, *J* = 7.6, 5.7, 1.4 Hz, bpy-5), 2.10 (18H, s,  $C_6(CH_3)_6$ ), 2.05 (3H, s,  $NCCH_3$ ). ESI-MS (*m/z*, acetonitrile): 230.6, [M]<sup>2+</sup> (calcd: 230.6). Anal. Calcd for  $C_{24}H_{29}F_{12}N_3P_2Ru$ : C, 38.41; H, 3.89; N, 5.60. Found: C, 38.57; H, 3.77; N, 5.65.

**Measurement of Redox Potentials.** To determine redox potentials of hydride complexes and hydride acceptors, voltammograms were recorded by cyclic and Osteryoung square wave voltammetry (CV and OSWV, respectively) with use of a BAS-100B (Bioanalytical Systems) or CHI604D (CH Instruments) electrochemical analyzer in deaerated acetonitrile with TBAH (0.1 M) as a supporting electrolyte under argon atmosphere at 298 ± 5 K. A standard three-electrode cell was used, which consists of a glassy carbon electrode (3 mm in diameter), a platinum wire, and Ag/AgNO<sub>3</sub> (0.01 M) in TBAH acetonitrile solution for working, counter, and reference electrode, respectively. The ferrocenium/ferrocene ( $Fc^+/Fc$ ) redox couple was measured as a secondary standard.<sup>14</sup> For the hydride complex, a high scan rate (>0.8 V/s) in CV, high SW frequency (>30 Hz) in OSWV, and careful polishing of the working electrode were required for acquisition of reproducible voltammograms. For aqueous solution, a stationary mercury drop (surface area ~1 mm<sup>2</sup>) prepared by EG&G PARC 303A SMDE was used as the working electrode. Errors for potentials reported are 10–20 mV. For variable temperature experiments, an ethanol-ice bath was used.

**Na-Hg Reduction.** A small amount of solid  $[Ru(tpy)(bpy)(NCCH_3)](PF_6)_2$  (<0.5 mg), for example, was placed in homemade glassware equipped with an optical cell. Sodium amalgam (Na-Hg, 0.5% Na in Hg) was placed in a compartment separated from the main compartment by a frit, and dry acetonitrile was vacuum-transferred to the glassware, which was then flame-sealed. Generation of the reduced species was achieved by gradually bringing small amounts of the solution into and out of contact with the amalgam, while monitoring the UV-vis absorption spectral changes.

**Reactions of the Hydride Complexes with Hydride Acceptors in Acetonitrile.** All solutions were handled either under argon or under vacuum and protected from ambient light. The Ru(II) hydrides are sensitive to carbon dioxide in air. Hydride complex (e.g., 7 mM) and hydride acceptor (A<sup>+</sup>, e.g., 10 mM) were dissolved in acetonitrile-*d*<sub>3</sub> (0.65 mL) in an NMR tube equipped with a J-Young valve under Ar. The time course of the reaction was followed by measurement of <sup>1</sup>H NMR spectra on a Bruker 400 MHz spectrometer at 298 ± 5 K. Chemical shifts ( $\delta$ ) of <sup>1</sup>H were recorded relative to residual protons in acetonitrile-*d*<sub>3</sub> (1.94 ppm). Integrations of peaks in these spectra were taken relative to THF or toluene, which were added as internal standard. Species in the solution were characterized by ESI-MS (Thermo-Finnigan LCQ Advantage) as necessary. When reaction was observed, the rate constant(s) were determined. In the case of a reaction requiring days to reach the end or the equilibrium, the final spectra normally indicated small amounts of decomposition. The presence of

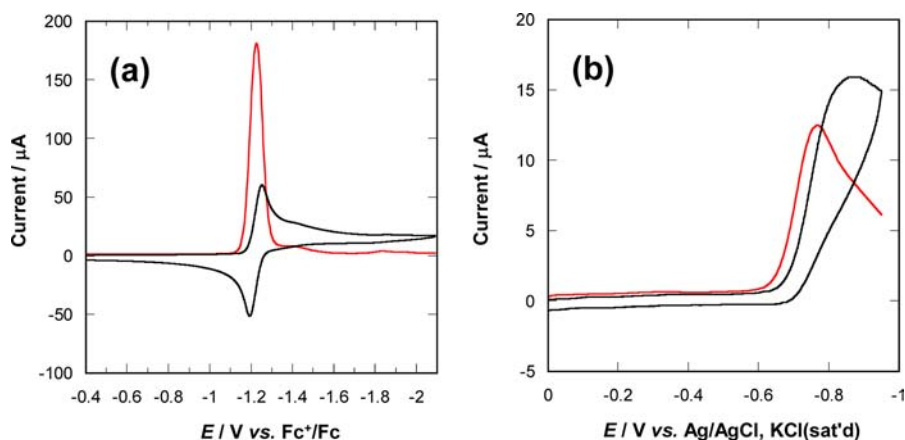


**Figure 1.** (a) Cyclic (black) and Osteryoung square wave (OSW) (red) voltammograms of 1 mM  $[\text{Ru}(\eta^6\text{-C}_6\text{Me}_6)(\text{bpy})(\text{NCCH}_3)]^{2+}$  in acetonitrile containing 0.1 M TBAH with 0.1 V/s scan rate (CV) and SW frequency of 15 Hz (OSWV). (b) Cyclic and OSW voltammograms for  $[\text{Ru}(\eta^6\text{-C}_6\text{Me}_6)(\text{bpy})(\text{OH}_2)]^{2+}$  in aqueous sodium phosphate buffer ( $\mu = 0.1$  M, pH 6.8) at scan rate 0.1 V/s (CV) and SW frequency of 15 Hz (OSWV) using glassy carbon as working electrode.

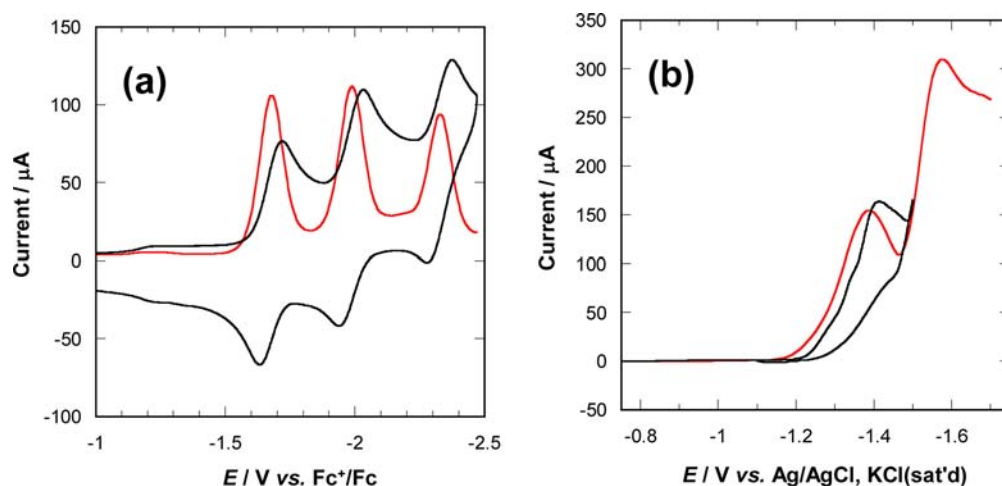


**Figure 2.** (a) CV (black) and OSWV (red) of 1 mM  $[\text{Ru}(\text{tpy})(\text{bpy})(\text{NCCH}_3)]^{2+}$  in acetonitrile containing 0.1 M TBAH at scan rate 0.8 V/s (CV) and SW frequency 120 Hz (OSWV). (b) Cyclic and OSW voltammograms for  $[\text{Ru}(\text{tpy})(\text{bpy})(\text{OH}_2)]^{2+}$  in aqueous sodium phosphate buffer ( $\mu = 0.1$  M, pH 6.8) at scan rate 0.1 V/s (CV) and SW frequency of 15 Hz (OSWV) using a Hg drop as working electrode.

decomposition products (including a hydrido bridged species in the case of  $\text{A}^+ = \text{BzIm}^+$ , Supporting Information, Figure S5) lowered the accuracy of the desired concentrations. Detailed treatment of the kinetic data is described in the Supporting Information.

**Computational Studies.** Calculations were carried out using the Gaussian 09 suite of programs.<sup>45</sup> DFT calculations were performed using the B3LYP hybrid functional,<sup>46–50</sup> the ECP28MWB(1f,0g) basis for Ru,<sup>51,52</sup> and the 6-31+G(d,p) basis for C, N, and H.<sup>53–58</sup> Geometry optimizations and vibrational frequency calculations were carried out in a PCM treatment<sup>59–61</sup> of the acetonitrile solvent using UAHF radii. The properties of the  $[\text{Ru}(\text{tpy})(\text{bpy})(\text{NCCH}_3)_n]^{2+}$  complexes for  $n = 1$  and 0 and  $z = 2, 1,$  and 0 were calculated using density functional theory, and the issue of the spin multiplicity of  $[\text{Ru}(\text{tpy})(\text{bpy})]^{0}$  was also explored using MP2 calculations that represent the interaction of spatially separated electrons more accurately than standard DFT.

## RESULTS

**Electrochemical Measurements.** The results of the electrochemical measurements are summarized in Table 1. In cyclic voltammetry of  $[\text{Ru}(\eta^6\text{-C}_6\text{Me}_6)(\text{bpy})(\text{NCCH}_3)]^{2+}$ , only one reversible reduction wave was observed. The reversibility of the reduction wave was confirmed to be Nernstian by applying the Randles–Sevcik equation to the scan-rate dependence of the

cathodic peak current,  $i_{pc}$ , (0.05–0.21 V/s, Supporting Information, Figure S1) using a diffusion coefficient of  $(1.1 \pm 0.2) \times 10^{-5}$   $\text{cm}^2/\text{s}$  for  $[\text{Ru}(\eta^6\text{-C}_6\text{Me}_6)(\text{bpy})(\text{NCCH}_3)]^{2+}$  determined by a  $^1\text{H}$  2D-DOSY experiment (Supporting Information, Figure S3), and the number of electrons involved was confirmed to be two. At higher scan rate ( $>1$  kV/s), the shape of the cathodic peak broadened compared with that of the corresponding anodic peak, but it did not split up into two peaks (Supporting Information, Figure S14).

The behavior found for  $[\text{Ru}(\eta^6\text{-C}_6\text{Me}_6)(\text{bpy})(\text{NCCH}_3)]^{2+}$  (Figure 1) is simpler than, but consistent with, that earlier reported for the chloro complex by Kaim et al.<sup>62</sup> and analogous 1,10-phenanthroline complexes reported by Stepnicka et al.<sup>63</sup> The fact that a two-electron process is observed implies that the reduction potential for  $[\text{Ru}(\eta^6\text{-C}_6\text{Me}_6)(\text{bpy})(\text{NCCH}_3)_n]^{+/0}$  ( $n = 1$  or 0) lies positive of that for  $[\text{Ru}(\eta^6\text{-C}_6\text{Me}_6)(\text{bpy})(\text{NCCH}_3)_n]^{2+/+}$  (the solvation of the reduced species will be discussed later) and cannot be exactly determined in this study.

In contrast to the two-electron reduction observed for  $[\text{Ru}(\eta^6\text{-C}_6\text{Me}_6)(\text{bpy})(\text{NCCH}_3)]^{2+}$ , the reduction of  $[\text{Ru}(\text{tpy})(\text{bpy})(\text{NCCH}_3)]^{2+}$  in acetonitrile (Figure 2) is dominated by one-

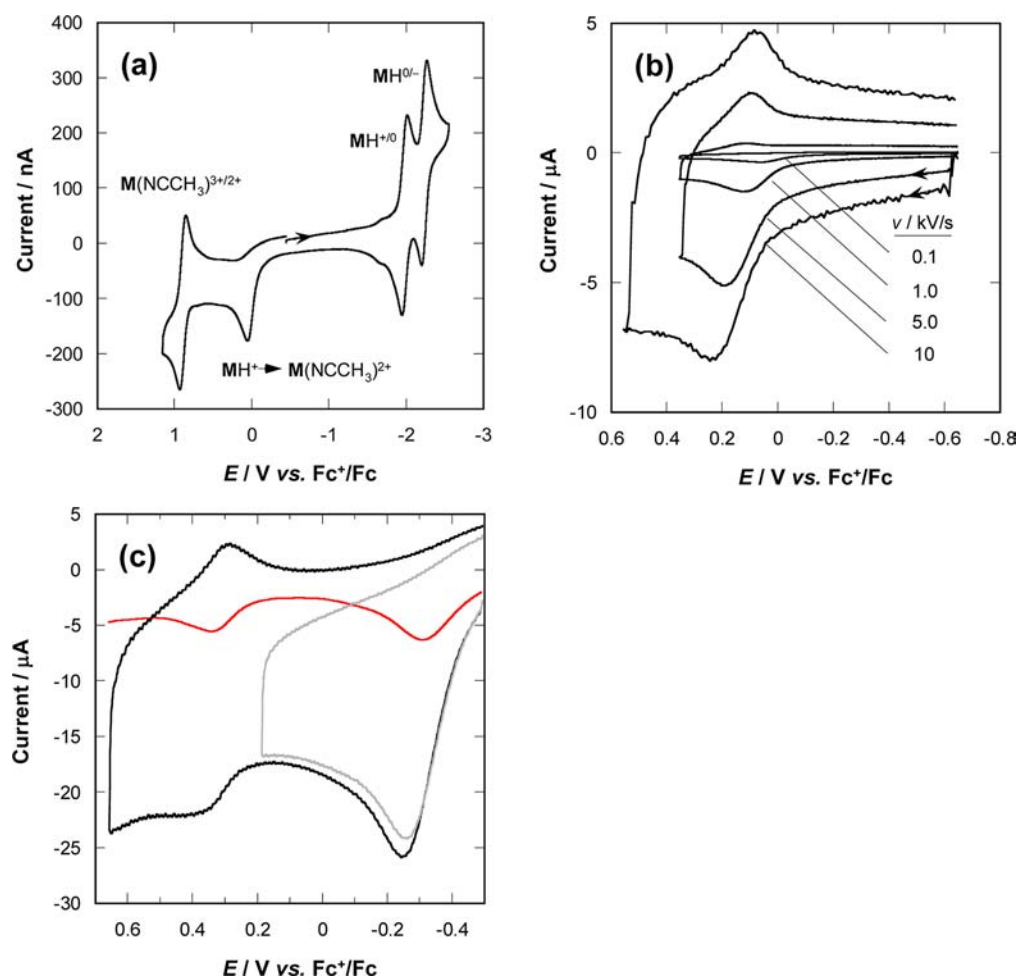


**Figure 3.** Cyclic voltammograms of  $[\text{Ru}(\text{tpy})(\text{bpy})\text{H}]^+$  ( $\text{MH}^+$ , 5 mM) in an acetonitrile solution containing TBAH (0.6 M), purged with argon (a) at scan rate of 25 V/s and (b) at various scan rates of more than 0.1 kV/s. A microelectrode (carbon fiber, 18  $\mu\text{m}$ ) was used as the working electrode. (c) Cyclic (black and gray) and OSWV (red) of 0.5 mM  $[\text{Ru}(\text{tpy})(\text{bpy})\text{H}]^+$  in TBAH (0.1 M) acetonitrile solution purged with argon. Scan rate 0.8 V/s (CV) and SW frequency 30 Hz (OSWV).

electron (confirmed at first reduction wave; see Supporting Information, Figure S2) and ligand-centered (tpy, tpy, and bpy) processes, which are chemically reversible at rapid scan rates ( $\geq 0.8$  V/s). The behavior found is in good agreement with previous work.<sup>37,64</sup> The second and third reduction waves were observed as irreversible waves at lower scan rates. Analysis of peak currents for the second reduction indicates that at sweep rates below 0.1 V/s, the anodic peak current becomes much less than its cathodic predecessor. This is consistent with acetonitrile loss from  $[\text{Ru}(\text{tpy})(\text{bpy})(\text{NCCH}_3)]^0$  on the time scale of  $\sim 0.1$  s.

Cyclic voltammetry (CV) of  $[\text{Ru}(\text{tpy})(\text{bpy})\text{H}]^+$  in acetonitrile is summarized in Figure 3 for a range of conditions. As previously reported,<sup>37</sup>  $[\text{Ru}(\text{tpy})(\text{bpy})\text{H}]^+$  undergoes chemically irreversible oxidation (Figure 3). The more cathodic peak was reported earlier, but not assigned.<sup>37</sup>

We note that it is not due to oxidation of  $[\text{Ru}(\text{tpy})(\text{bpy})(\text{NCCH}_3)]^{2+}$ , which occurs at  $\sim +0.9$  V in Figure 3a. This peak is notably absent in Figure 3c. Reactions following oxidation of  $d^6$  hydrides are complex.<sup>65,66</sup> Tillet reports bimolecular disproportionation of the one-electron oxidation product, followed by proton loss from the doubly oxidized species, with the parent hydride serving as a proton acceptor to give a dihydrogen complex. Conceivably the peak is due to oxidation of  $[\text{Ru}(\text{tpy})(\text{bpy})(\text{NCCH}_3)]^{2+}$  to  $[\text{Ru}(\text{tpy})(\text{bpy})(\text{NCCH}_3)]^{3+}$  or

to the dihydrogen complex  $[\text{Ru}(\text{tpy})(\text{bpy})(\text{H}_2)]^{2+}$  formed by reaction of the parent hydride complex  $[\text{Ru}(\text{tpy})(\text{bpy})\text{H}]^+$  with the very strong acid  $[\text{Ru}(\text{tpy})(\text{bpy})\text{H}]^{3+}$ . In water,  $[\text{Ru}(\text{tpy})(\text{bpy})(\text{H}_2)]^{2+}$  formed by proton transfer from  $\text{H}_3\text{O}^+$  is converted to  $[\text{Ru}(\text{tpy})(\text{bpy})(\text{OH}_2)]^{2+} + \text{H}_2$  with  $k_{\text{obs}} \sim 4 \text{ s}^{-1}$  at room temperature.<sup>10</sup>

Oxidation of  $[\text{Ru}(\eta^6\text{-C}_6\text{Me}_6)(\text{bpy})\text{H}]^+$  occurs at +0.32 V vs  $\text{Fc}^+/\text{Fc}$  (Supporting Information, Figure S6). Although we attempted to observe reversibility on this oxidation wave, we could not do that even at a scan rate of 10 kV/s.

**Electronic Spectra of the Reduced Complexes.** The electronic absorption spectra obtained by sodium-amalgam reduction of  $[\text{Ru}(\eta^6\text{-C}_6\text{Me}_6)(\text{bpy})(\text{NCCH}_3)]^{2+}$  and  $[\text{Ru}(\text{tpy})(\text{bpy})(\text{NCCH}_3)]^{2+}$  in acetonitrile are shown in Figures 4 and 5, respectively. The latter may be compared with those for reduction of  $[\text{Ru}(\text{tpy})_2]^{2+}$  from the literature shown in Figure 5b.

The spectrum found for the  $\text{Ru}(\eta^6\text{-C}_6\text{Me}_6)(\text{bpy})$  compound (in agreement with the literature<sup>62</sup>) exhibits a typical bound bipyridine radical set of transitions that results from a direct *two-electron* reduction of the parent complex. Most interestingly Kaim<sup>62</sup> has shown that the reduction product  $[\text{Ru}(\eta^6\text{-C}_6\text{Me}_6)(\text{bpy})(\text{NCCH}_3)_n]^0$  is diamagnetic and suggested a significant contribution from a  $\text{Ru}^{\text{I}}(\text{bpy}^{\bullet-})$  resonance structure. This assignment is consistent with a generalized valence bond

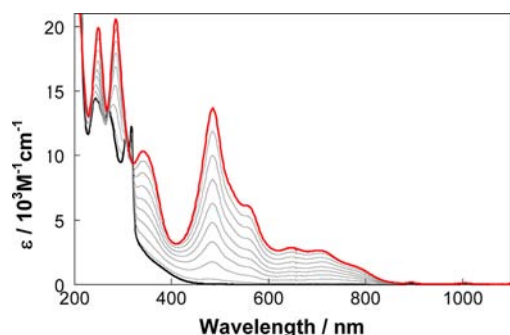


**Figure 4.** UV-vis absorption spectral changes during stepwise reduction of  $[\text{Ru}(\eta^6\text{-C}_6\text{Me}_6)(\text{bpy})(\text{NCCH}_3)]^{2+}$  by Na-Hg in  $\text{CH}_3\text{CN}$ : initial spectrum, black curve; fully reduced spectrum, red curve.

configuration interaction involving the sharing of a pair of electrons between the  $\pi$  and  $\pi^*$  orbitals resulting from the overlap of  $\text{Ru}(d\pi)$  and  $\text{bpy}(\pi^*)$  orbitals. By contrast, in the case of the terpyridyl complex, the similarities between parts a and b of Figure 5 indicate that the HOMO has significant electron density in terpyridyl-based orbitals. The cyclic voltammetric response also suggests that the two sequential one-electron reductions are ligand centered.

**Computational Studies.** Computational results for  $[\text{Ru}(\text{tpy})(\text{bpy})(\text{NCCH}_3)_n]^{z+}$  ( $z = 2, 1,$  and  $0$ ) are presented in Table 2. Details of the absolute electronic energies, enthalpies, and free energies of the various species are provided in the Supporting Information (Table S5). The calculated hydricity,  $\text{p}K_{\text{a}}$ , and bond-dissociation free energy (BDFE) values of  $[\text{Ru}(\text{tpy})(\text{bpy})\text{H}]^+$  listed in Table 2 will be used for comparison with experimental estimates below.

We should note that, while the choice of the spin state is obvious for the +2 and +1 charged Ru complexes, this is not the case for the 0 charge species. Meyer et al.<sup>68</sup> have reported that gas-phase DFT calculations predict a triplet state with one unpaired electron on the tpy ligand and the other on the bpy ligand to be 77 kcal/mol lower than the closed-shell singlet state. The density functional employed in that work, however, would underestimate the interaction between these two spatially separated electrons. They also assumed a molecule of acetonitrile occupying the sixth coordination site. We have used MP2 calculations in which the exchange interaction between these two (and all other) electrons is treated accurately. We have

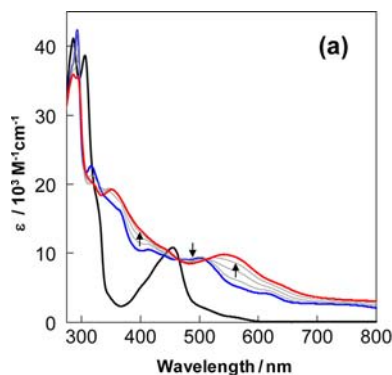


**Table 2. Results for DFT Calculations of  $\text{p}K_{\text{a}}$  and Bond-Dissociation Free Energy of  $[\text{Ru}(\text{tpy})(\text{bpy})\text{H}]^+$**

| reaction  | $n$ | $\text{p}K_{\text{a}}$ | BDFE <sup>a</sup> | $\Delta G^{\circ a}$ |
|---|-----|------------------------|-------------------|----------------------|
| $[\text{Ru}(\text{tpy})(\text{bpy})\text{H}]^+ + n\text{CH}_3\text{CN}(\text{l}) \rightarrow$ | 0   | 35.2                   |                   |                      |
| $[\text{Ru}(\text{tpy})(\text{bpy})(\text{NCCH}_3)_n]^0 + \text{H}^+(\text{s})$               | 1   | 42.6                   |                   |                      |
| $[\text{Ru}(\text{tpy})(\text{bpy})\text{H}]^+ + n\text{CH}_3\text{CN}(\text{l}) \rightarrow$ | 0   |                        | 64.3              |                      |
| $[\text{Ru}(\text{tpy})(\text{bpy})(\text{NCCH}_3)_n]^+ + \text{H}^+(\text{s})$               | 1   |                        | 59.6              |                      |
| $[\text{Ru}(\text{tpy})(\text{bpy})(\text{NCCH}_3)]^{2+} \rightarrow$                         |     |                        |                   | 12.7                 |
| $[\text{Ru}(\text{tpy})(\text{bpy})]^{2+} + \text{CH}_3\text{CN}(\text{l})$                   |     |                        |                   |                      |
| $[\text{Ru}(\text{tpy})(\text{bpy})(\text{NCCH}_3)]^+ \rightarrow$                            |     |                        |                   | 4.9                  |
| $[\text{Ru}(\text{tpy})(\text{bpy})]^+ + \text{CH}_3\text{CN}(\text{l})$                      |     |                        |                   |                      |
| $[\text{Ru}(\text{tpy})(\text{bpy})(\text{NCCH}_3)]^0 \rightarrow$                            |     |                        |                   | -10.0                |
| $[\text{Ru}(\text{tpy})(\text{bpy})]^0 + \text{CH}_3\text{CN}(\text{l})$                      |     |                        |                   |                      |

<sup>a</sup>In kcal/mol.

performed these calculations on the same six-coordinate complex at the optimized singlet geometry at the B3LYP level of theory, and the results indicate that the closed-shell singlet state is 39.1 kcal/mol more stable than the triplet state at the UMP2 level and 3.6 kcal/mol more stable than the triplet state at the spin-projected PMP2 level of theory. The doubly occupied HOMO of the singlet state in the MP2 calculations is mostly a  $\pi^*$  orbital localized on two of the three py rings in the tpy, with a small contribution from a Ru  $d\pi$  orbital (Figure 6).

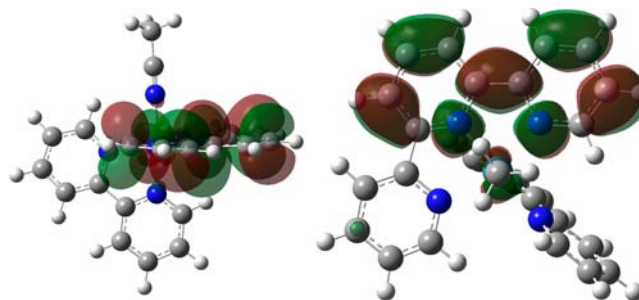


**Figure 6.** The doubly occupied HOMO of the singlet MP2 state of  $[\text{Ru}(\text{tpy})(\text{bpy})(\text{NCCH}_3)]^0$ . The view on the left is approximately perpendicular to the plane of the bpy ligand; the view on the right is approximately along the axis containing the Ru center and the heavy atoms of the acetonitrile ligand and shows that the  $\pi^*$  orbital on the tpy ligand is localized on only two of its three rings.

**Acidity Determinations.** The hydride complex  $[\text{Ru}(\eta^6\text{-C}_6\text{Me}_6)(\text{bpy})\text{H}]^+$  is readily deprotonated by tetramethylguan-

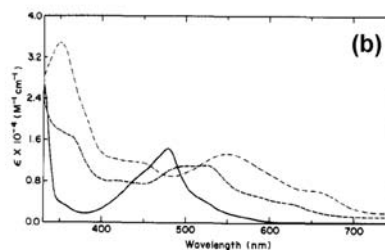


**Figure 5.** UV-vis absorption spectral changes during stepwise reduction of (a)  $[\text{Ru}(\text{tpy})(\text{bpy})(\text{NCCH}_3)]^{2+}$  (black to blue and then red) and (b) of  $[\text{Ru}(\text{tpy})_2]^{2+}$  (solid line) to  $[\text{Ru}(\text{tpy})_2]^+$  (---) and  $[\text{Ru}(\text{tpy})_2]^0$  (- · -) in DMF from the literature.<sup>67</sup> Reprinted with permission from ref 67. Copyright 1988 American Chemical Society.

dine in acetonitrile with formation of an equilibrium mixture (eq 7; Supporting Information, Figure S7A). The equilibrium constant  $K_7 = 6.2 \pm 0.5$  ( $\Delta pK_a$  of  $0.8 \pm 0.1$ ) was calculated by integration of the  $^1\text{H}$  NMR spectra (Figure 7). The subtraction

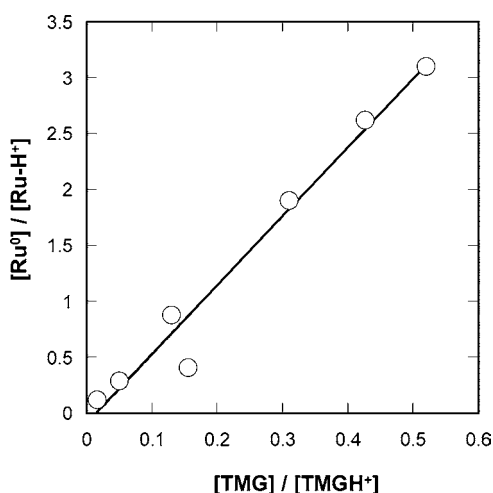
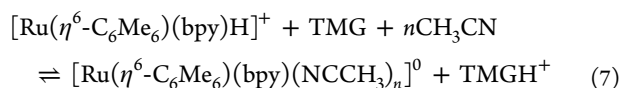


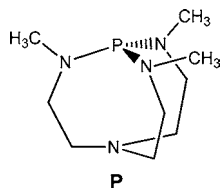
**Figure 7.** The ratio  $[\{\text{Ru}(\eta^6\text{-C}_6\text{Me}_6)(\text{bpy})(\text{NCCH}_3)_n\}^0]/[\{\text{Ru}(\eta^6\text{-C}_6\text{Me}_6)(\text{bpy})\text{H}\}^+]$  plotted as a function of  $[\text{TMG}]/[\text{TMGH}^+]$ .

of  $\Delta pK_a$  from the  $pK_a$  of  $\text{TMGH}^+$  ( $23.3$ )<sup>69</sup> gives a  $pK_a$  of  $22.5 \pm 0.1$  for  $[\text{Ru}(\eta^6\text{-C}_6\text{Me}_6)(\text{bpy})\text{H}]^+$ . Thus, the hydricity for  $[\text{Ru}(\eta^6\text{-C}_6\text{Me}_6)(\text{bpy})\text{H}]^+$  was determined to be  $54 \pm 2$  kcal/mol from eq 1a using the  $pK_a$  and the two-electron reduction potential for  $[\text{Ru}(\eta^6\text{-C}_6\text{Me}_6)(\text{bpy})(\text{NCCH}_3)_2]^{2+}$ .



$[\text{Ru}(\text{tpy})(\text{bpy})\text{H}]^+$  is too weak to be deprotonated by TMG, and its  $pK_a$  is thus estimated as  $\gg 23.3$ . In fact,  $[\text{Ru}(\text{tpy})(\text{bpy})\text{H}]^+$  did react with the much stronger base **P**, one of the proazaphosphatranes (Chart 3;  $pK_a = 32.9$ <sup>70</sup>), in an acetonitrile-

**Chart 3.** Proazaphosphatranes Base

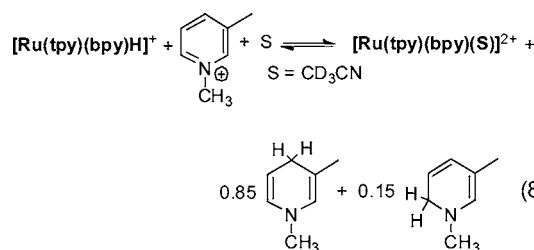


$d_3$  solution containing 3.8 mM hydride and base over several hours (Supporting Information, Figure S7B). Although the deuterated base  $\text{PD}^+$  ( $\delta_{\text{31P}} -10.1$  ppm, triplet,  $J = 77$  Hz) and the free base ( $\delta_{\text{31P}} 119.6$  ppm) were clearly observed in the  $^{31}\text{P}$  and  $^1\text{H}$  NMR spectra [while the protonated base  $\delta_{\text{31P}} -9.6$  ppm (singlet) was not], the deprotonated complex,  $[\text{Ru}(\text{tpy})(\text{bpy})(\text{NCCH}_3)_n]^0$ , was not detected, probably due to its instability and unknown resultant product(s).

#### Thermodynamics and Kinetics of Hydride Ion Transfer.

**A. Organics.** Because of its low acidity, the hydricity of  $[\text{Ru}(\text{tpy})(\text{bpy})\text{H}]^+$  in acetonitrile could not be determined via Scheme 1. Accordingly, we studied the reactions of this Ru(II) hydride with characterized organic hydride acceptors to evaluate equilibrium constants for the equilibria according to Scheme 2. Among the types of hydride acceptor compounds we tested, which are imidazolium,  $\text{NAD}^+$  model cations, as well as a  $W(0)$  carbonyl compound and Pt(II) complexes, only the organic compounds (see Chart 1) reacted with  $[\text{Ru}(\text{tpy})(\text{bpy})\text{H}]^+$  to give the expected free, hydride-transfer product. The hydride acceptors  $\text{A}^+$  studied are listed in Table 3 along with the hydricities of their conjugate donors  $\text{AH}$  ( $\Delta G_{\text{H}}^\circ(\text{AH})/\text{kcal mol}^{-1}$ ), reaction products, and hydride-transfer rate constants ( $k_f$ ) determined by  $^1\text{H}$  NMR in  $\text{CD}_3\text{CN}$ . To obtain the hydricities tabulated in Table 3, we used the thermo- and electrochemical data<sup>30</sup> and the cycle described in ref 71. Note that the hydricity enthalpies in the latter are incorrect systematically by  $-32.8$  kcal/mol because of the wrong sign used for the reduction potential of  $\text{TMPD}^{\bullet+}$  ( $N,N,N',N'$ -tetramethyl-*p*-phenylenediamine radical cation).<sup>71</sup> For details, see the Supporting Information.

Of the previously characterized hydride acceptors, only  $\text{DMpy}^+$  reacted at room temperature to give a quantifiable equilibrium mixture. The result, formed over the course of 1 week, was an 85:15 mixture of 1,4- and 1,6- $\text{DMpyH}$  (eq 8). An



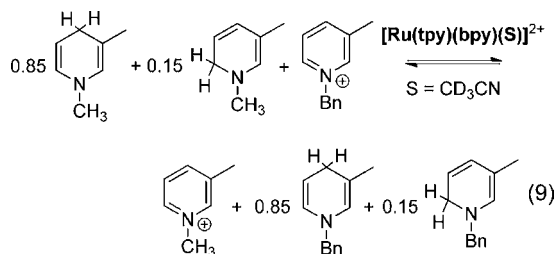
equilibrium constant of  $16.8 \pm 2.0$  was calculated for this reaction by integration of the  $^1\text{H}$  NMR spectra, which was in good agreement with the value calculated from the ratio of the forward and reverse rate constants ( $17.6 \pm 2.0$ ). The free-energy change for eq 8 is  $-1.7 \pm 0.2$  kcal/mol in acetonitrile- $d_3$ .

**Table 3.** Reaction of  $[\text{Ru}(\text{tpy})(\text{bpy})\text{H}]^+$  with Hydride Acceptors  $\text{A}^+$  (Chart 2) in  $\text{CD}_3\text{CN}$  at 298 K

| acceptor, $\text{A}^+$                | conjugate donor, $\text{AH}$           | $\Delta G_{\text{H}}^\circ(\text{AH})$ in kcal mol <sup>-1</sup> | product(s) observed                   | $10^3 k_f^a$ in M <sup>-1</sup> s <sup>-1</sup> |
|---------------------------------------|--|--|---------------------------------------|---|
| BzIm <sup>+</sup>                     | 1,2-BzImH                              | $45 \pm 3^{b,c,28}$  | 1,2-BzImH                             | $6.5 \pm 0.2$                                   |
| BMPy <sup>+</sup>                     | 1,4-BMPyH                              | $43 \pm 3^{b,30}$  | 1,4-BMPy (95%), 1,6-BMPy (5%)         | $(1.5 \pm 0.2) \times 10$                       |
| DMPy <sup>+</sup>                     | 1,4-DMPyH                              | $41 \pm 3^b$   | 1,4-DMPy (85%), 1,6-DMPy (15%)        | $1.6 \pm 0.2^d$                                 |
| $[\text{W}(\text{CO})_5(\text{S})]^e$ | $[\text{W}(\text{CO})_5\text{H}]^-$    | $40 \pm 2^{72}$  | $[\text{Ru}-\mu\text{-H}-\text{W}]^+$ | 0.5   |
| $[\text{Pt}(\text{depe})_2]^{2+}$     | $[\text{Pt}(\text{depe})_2\text{H}]^+$ | $44 \pm 2^{86}$  | no reaction                           |   |
| $[\text{Pt}(\text{dppe})_2]^{2+}$     | $[\text{Pt}(\text{dppe})_2\text{H}]^+$ | $53 \pm 2^{12}$  | no reaction                           |   |

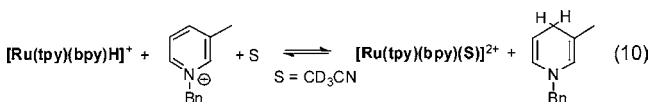
<sup>a</sup>A second-order rate constant of the hydride-transfer reaction from  $[\text{Ru}(\text{tpy})(\text{bpy})\text{H}]^+$  to an acceptor. See Experimental Section for details. <sup>b</sup>Determined here; see the text and the Supporting Information. <sup>c</sup>Assuming the same  $T\Delta S$  values as for  $\text{BMPy}^+$  and  $\text{DMPy}^+$  because of the similarity in their structures. <sup>d</sup>A second-order rate constant of the reverse reaction ( $k_r$ ) is  $(9.2 \pm 3.2) \times 10^{-5}$  M<sup>-1</sup> s<sup>-1</sup>. <sup>e</sup>S =  $\text{CH}_3\text{CN}$ .

When 1 equiv of  $\text{BMpy}^+$  was added to the equilibrium mixture, we also found formation of a new equilibrium mixture containing an 85:15 mixture of 1,4- and 1,6-BMpyH (Bn =  $-\text{CH}_2\text{Ph}$ , eq 9

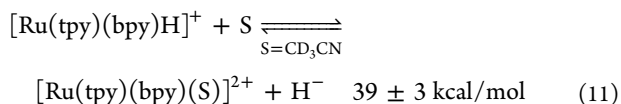


over 2 days, with an equilibrium constant of  $26.5 \pm 2.0$  as determined from the  $^1\text{H}$  NMR spectrum. [Note: To verify that this is an equilibrium reaction, additional  $\text{DMpy}^+$  was added to an equilibrated solution and the concentration of each species was confirmed to be that estimated from the equilibrium constant.] This equilibrium constant corresponds to a free-energy change of  $-1.9 \pm 0.2$  kcal/mol for eq 9.

Since the hydricity of 1,4-BMpyH is evaluated as  $43 \pm 3$  kcal/mol in acetonitrile as shown in Table 3, we related the hydricity of  $[\text{Ru}(\text{tpy})(\text{bpy})\text{H}]^+$  to that of this pyridinium by estimation of the free-energy change for the reaction of  $[\text{Ru}(\text{tpy})(\text{bpy})\text{H}]^+$  with  $\text{BMpy}^+$  (eq 10).



The free energy change  $\Delta G$  (eq 10) is estimated as the summation of two free energy changes described above, i.e.,  $-3.6$  kcal/mol with an uncertainty of about 1 kcal/mol, which is caused by errors in the two free energy changes and a minor contribution from the formation of 1,6-BMpyH in the reaction. [Note: The difference of hydricities between the 1,4- and 1,6-dihydro form of pyridinium cations is typically within a few kcal/mol.<sup>30,73</sup>] The magnitude of  $\Delta G_{\text{H}^-}^\circ$  for  $[\text{Ru}(\text{tpy})(\text{bpy})\text{H}]^+$  can then be estimated as  $39 \pm 3$  kcal/mol (eq 11) by addition of  $\Delta G$  (eq 10) to  $\Delta G_{\text{H}^-}^\circ = 43 \pm 3$  kcal/mol for 1,4-BMpyH.

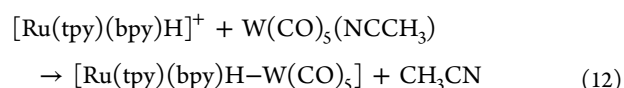


This value is consistent with the hydricity of  $[\text{HCO}_2]^-$ , which is estimated as in the range between 51 and 44 kcal/mol<sup>3,86</sup>, i.e.,  $47 \pm 4$  kcal/mol or reported as  $43 \pm 2$  kcal/mol,<sup>74</sup> since  $\text{CO}_2$  yields the formate complex upon reaction with  $[\text{Ru}(\text{tpy})(\text{bpy})\text{H}]^+$  in acetonitrile.<sup>37</sup>

As detailed in Table 3, the reaction of  $[\text{Ru}(\text{tpy})(\text{bpy})\text{H}]^+$  with  $\text{BMPy}^+$  and  $\text{DMPy}^+$  produces 1,4- and 1,6-dihydropyridine isomers, an observation consistent with results obtained in Ishitani's laboratory.<sup>75</sup> In addition, with the three acceptors studied here, we detected intermediate species (Supporting Information, Figures S8 and S9), attributed to  $\eta^2$ -imidazole and  $\eta^2$ -dihydropyridine complexes.<sup>75</sup> For example, with  $\text{BzIm}^+$ , the bpy-6H resonance of the hydride ( $\delta$  9.75 ppm) decreased while the corresponding resonance of the acetonitrile complex ( $\delta$  9.60) increased. A broad peak at  $\delta$  7.35 grew in with time, finally narrowing to a triplet after about 2 days. The  $\delta$  7.35 ppm resonance was observed with both L = bpy and L = dnb (dnb = 4,4'-dinonyl-2,2'-bipyridine). The presence of an intermediate

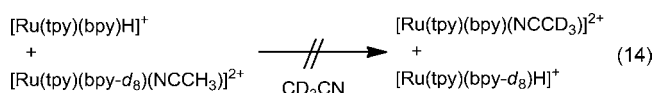
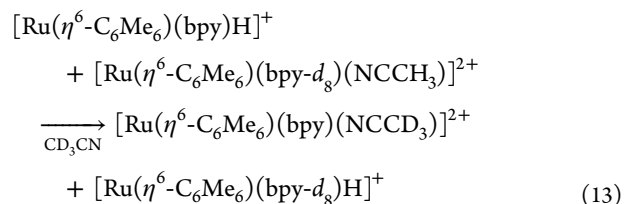
was also indicated by ESI-MS of the solution 2 h after mixing;  $m/z = 679.7$  [ $[\text{Ru}(\text{tpy})(\text{bpy})(\text{BzImH})(\text{CH}_3\text{CN}) - \text{H}^+]^+$ ].

**B.1. Metal-Centered Hydride Acceptors:  $\text{W}(\text{CO})_5(\text{NCCH}_3)$ .** For the case of  $\text{W}(\text{CO})_5(\text{NCCH}_3)$  as hydride ion acceptor, a hydride ion bridged species formed over 1 day [ $\delta_{\text{H}} -21$  ppm, intense singlet with weak doublet,  $J(^{183}\text{W}-^1\text{H}) = 44$  Hz. IR ( $\text{cm}^{-1}$ , acetonitrile):  $\nu_{\text{CO}}$  2062 (w), 1922 (s), 1896 (sh)] and remained constant after about 3 days. In contrast to other results,<sup>72</sup> there is no evidence for formation of a formyl product and the position of the chemical shift of the new hydride resonance is consistent with the hydride-bridged description. No mononuclear  $[\text{W}(\text{CO})_5\text{H}]^-$  ( $\delta_{\text{H}} -4.2$  ppm)<sup>76</sup> was observed. From the proton NMR data, the rate constant for eq 12 is ca.  $0.5 \times 10^{-3} \text{ M}^{-1} \text{ s}^{-1}$  (Supporting Information, Figure S10).

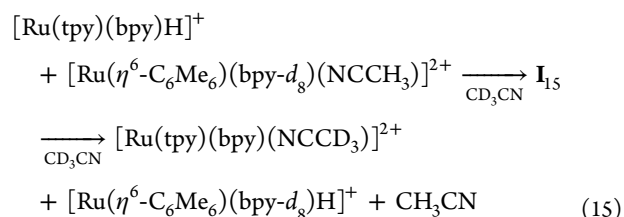


**B.2.  $[\text{Pt}(\text{dppe})_2]^{2+}$  Acceptor.**  $[\text{Ru}(\eta^6\text{-C}_6\text{Me}_6)(\text{bpy})\text{H}](\text{OTf})$  was found to react with 1 equiv of  $[\text{Pt}(\text{dppe})_2]^{2+}$ , for which  $\Delta G_{\text{H}^-}^\circ = 52.5$  kcal/mol<sup>12</sup> in acetonitrile- $d_3$ , and reduced one-third of the Pt complex to  $[\text{Pt}(\text{dppe})_2\text{H}]^+$  over the course of 30 days. Unfortunately, this reaction was accompanied by side reactions to give two unknown  $\text{Ru}(\eta^6\text{-C}_6\text{Me}_6)$  complexes, potentially  $[\text{Ru}(\eta^6\text{-C}_6\text{Me}_6)(\text{bpy})(\text{OTf})]^+$  besides  $[\text{Ru}(\eta^6\text{-C}_6\text{Me}_6)(\text{bpy})(\text{NCCH}_3)]^{2+}$ . However, the hydricity of  $[\text{Ru}(\eta^6\text{-C}_6\text{Me}_6)(\text{bpy})\text{H}]^+$  could be estimated as  $\geq 52.5$  kcal/mol, because 30% of the Ru hydride complex still remained when no further changes in the  $^1\text{H}$  NMR spectrum could be observed.

**B.3. Ru(II) Acceptors.** We examined the possibility of hydride ion self-exchange (eqs 13 and 14) by incorporating bpy- $d_8$  into the acetonitrile complex, i.e.,



For  $[\text{Ru}(\eta^6\text{-C}_6\text{Me}_6)(\text{bpy})\text{H}]^+$  (eq 13), reaction was complete in  $<15$  min with 6.3 mM initial concentration of hydride and acetonitrile complexes. This leads to an estimate of  $k_{13} > 1 \text{ M}^{-1} \text{ s}^{-1}$ ; no intermediate species were observed. For  $[\text{Ru}(\text{tpy})(\text{bpy})\text{H}]^+$  (eq 14), no reaction was found even after 18 days, imposing an upper limit of  $k_{14} \leq 3 \times 10^{-6} \text{ M}^{-1} \text{ s}^{-1}$  when assuming 3% reaction.



The great contrast in the rate constants for eqs 13 and 14 led us to examine the "cross" reaction (eq 15). We observed the rapid (estimated rate constant  $> 4 \times 10^{-1} \text{ M}^{-1} \text{ s}^{-1}$  at 298 K) formation of an intermediate  $\text{I}_{15}$  complex and followed the kinetics ( $k_{\text{soln}} =$

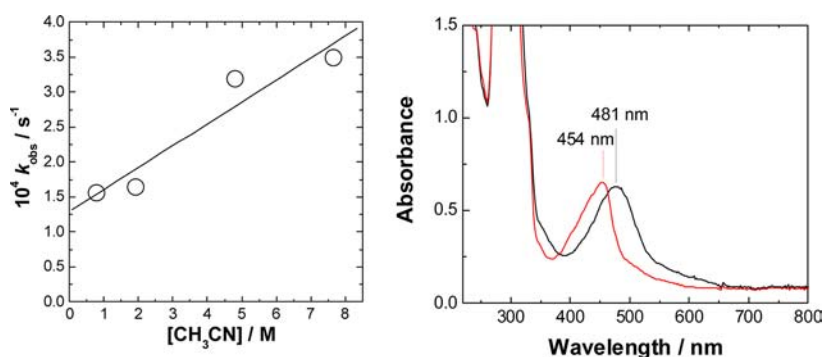


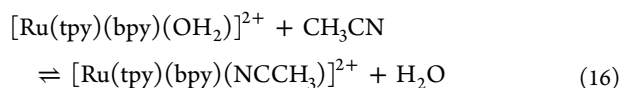
**Figure 8.** (Left) Pseudo-first-order rate constant for the substitution reaction (eq 16) as a function of the concentration of incoming ligand acetonitrile [slope  $(3.1 \pm 0.7) \times 10^{-5} \text{ M}^{-1} \text{ s}^{-1}$ , intercept  $(1.3 \pm 0.3) \times 10^{-4} \text{ s}^{-1}$ ]. (Right) Spectral changes observed on conversion of  $[\text{Ru}(\text{tpy})(\text{bpy})(\text{OH}_2)]^{2+}$  (black trace) to  $[\text{Ru}(\text{tpy})(\text{bpy})(\text{NCCH}_3)]^{2+}$  (red trace) in 10–40% acetonitrile–water (eq 16).

### Scheme 3. Acidity Estimation in Acetonitrile ( $\text{M} = \text{Ru}(\text{tpy})(\text{bpy})$ )

| Reaction   | $\Delta G^\circ$ , kcal/mol  |
|--|--|
| $\text{MH}^+ + \text{CH}_3\text{CN} \rightarrow \text{M}(\text{NCCH}_3)^{2+} + \text{H}^-$ | $\Delta G_{\text{H}}^\circ = 39 \pm 3$   |
| $\text{M}(\text{NCCH}_3)^{2+} + 2\text{e}^- \rightarrow \text{M}(\text{NCCH}_3)^0$         | $-2FE^\circ(2+/0) = 84.2$ , ( $E^\circ = -1.83 \text{ V vs Fc}^+/ \text{Fc}$ ) |
| $\text{H} \rightarrow \text{H}^+ + 2\text{e}^-$  | $-79.6 \text{ vs Fc}^+/\text{Fc}^{16}$   |
| $\text{MH}^- + \text{CH}_3\text{CN} \rightarrow \text{M}(\text{NCCH}_3)^0 + \text{H}^+$    | $\Delta G_{\text{H}}^\circ = 44 \pm 3$   |

$7.5 \times 10^{-4} \text{ s}^{-1}$  at 298 K;  $\Delta H^\ddagger = 16 \pm 1 \text{ kcal/mol}$  and  $\Delta S^\ddagger = -20 \pm 2 \text{ cal/mol}\cdot\text{K}$  between 265 and 310 K from an Eyring plot; see Supporting Information, Figure S15) of its decomposition to the above products. The intermediate  $\text{I}_{15}$  is a  $\mu\text{-H}$  bridged complex based on comparison of the position of its  $^1\text{H}$  NMR hydride resonance ( $\delta -21.9 \text{ ppm}$ ) with those of known bridged species.<sup>77,78</sup> Preliminary UV–vis experiments in water provided a lower limit of  $10^1 \text{ M}^{-1} \text{ s}^{-1}$  for reaction of  $[\text{Ru}(\text{tpy})(\text{bpy})\text{H}]^+$  and  $[\text{Ru}(\eta^6\text{-C}_6\text{Me}_6)(\text{bpy})(\text{OH}_2)]^{2+}$  in water.<sup>79</sup>

For  $[\text{Ru}(\eta^6\text{-C}_6\text{Me}_6)(\text{bpy})\text{H}]^+$  (eq 15), the disruption of the bridged dimer, if formed, must proceed with a rate constant  $>10^{-3} \text{ s}^{-1}$  based on the time elapsed between preparation of the solution and the first NMR observation. As noted above, for  $\text{I}_{15}$  the disruption of the asymmetric bridged species at the  $\text{Ru}(\text{tpy})$  site is  $7.5 \times 10^{-4} \text{ s}^{-1}$  at 298 K. Such rate constants are qualitatively consistent with rates of ligand loss found for formate and acetonitrile complexes in aqueous media: For formate loss from  $[\text{Ru}(\eta^6\text{-C}_6\text{Me}_6)(\text{bpy})(\text{HCO}_2)]^+$  the rate constant is  $(3 \pm 1) \times 10^{-3} \text{ s}^{-1}$  while for  $[\text{Ru}(\text{tpy})(\text{bpy})(\text{HCO}_2)]^+$  the analogous rate constant is  $2 \times 10^{-4} \text{ s}^{-1}$  in water.<sup>9</sup> In 10–40% acetonitrile–water the substitution reaction (eq 16) proceeds with  $k_{\text{f}} = (3.1 \pm 0.7) \times 10^{-5} \text{ M}^{-1} \text{ s}^{-1}$  and  $k_{\text{r}} = (1.3 \pm 0.3) \times 10^{-4} \text{ s}^{-1}$  (Figure 8). The data gathered in connection with eq 16 (with standard state for water as solvent  $K = 0.24 \pm 0.08 \text{ M}^{-1}$ ; including the fact that water is 55 M gives  $K = 13 \pm 4$ ) will also be of interest later when solvent contributions to the thermodynamics of hydricity will be discussed.



## DISCUSSION

### Coordination Numbers of the Reduced Complexes.

One remarkable realization, based on the UV–vis spectroscopy in acetonitrile, is that both  $[\text{Ru}(\eta^6\text{-C}_6\text{Me}_6)(\text{bpy})(\text{NCCH}_3)]^0$

and  $[\text{Ru}(\text{tpy})(\text{bpy})(\text{NCCH}_3)]^0$  contain reduced polypyridyl ligands, bpy and tpy, respectively. In the case of the former, this conclusion is also supported by the prior work of Kaim et al.<sup>62</sup> However, coordination numbers of the reduced complexes are still unclear. For  $[\text{Ru}(\text{tpy})(\text{bpy})(\text{NCCH}_3)]^0$  the substitution kinetics of  $\text{CO}_2$  binding<sup>68</sup> indicate that  $n = 1$ ; i.e.,  $[\text{Ru}(\text{tpy})(\text{bpy})(\text{NCCH}_3)]^0$  is the dominant form on the cyclic voltammetric time scale of less than 1 s, confirmed by our observation indicating that acetonitrile loss from  $[\text{Ru}(\text{tpy})(\text{bpy})(\text{NCCH}_3)]^0$  is on the time scale of  $\sim 0.1 \text{ s}$ . Thus, electrochemical potentials measured in this study reflect those for  $n = 1$  for both the singly and doubly reduced species. These assignments are supported by DFT calculation: (1) according to Table 2, the calculated free-energy changes for loss of acetonitrile are +12.7, +4.9, and  $-10.0 \text{ kcal/mol}$  from  $z = 2, 1$ , and 0, respectively, and (2) comparison of experimental (Figure 5) and calculated electronic spectra (Supporting Information, Figure S12) for doubly reduced species is consistent with this conclusion.

Less information is available for  $[\text{Ru}(\eta^6\text{-C}_6\text{Me}_6)(\text{bpy})(\text{NCCH}_3)]^0$ : Kaim has shown that  $\text{Cl}^-$  is lost upon electrochemical reduction of  $[\text{Ru}(\eta^6\text{-C}_6\text{Me}_6)(\text{bpy})\text{Cl}]^+$  and assumed that  $n = 0$  is the dominant form of the doubly reduced species.<sup>62</sup> In our CV measurement for  $[\text{Ru}(\eta^6\text{-C}_6\text{Me}_6)(\text{bpy})(\text{NCCH}_3)]^{2+}$  at high scan rate ( $>1 \text{ kV/s}$ , Supporting Information, Figure S14), although we could not observe a splitting of the one cathodic peak involving two-electron reduction at lower scan rate into two peaks, the broadened peak (compared with the anodic peak) indicates that  $n = 0$ ; i.e.,  $[\text{Ru}(\eta^6\text{-C}_6\text{Me}_6)(\text{bpy})]^0$  and probably  $[\text{Ru}(\eta^6\text{-C}_6\text{Me}_6)(\text{bpy})]^+$  are the dominant forms on the time scale of more than 1 ms. Thus, in the case of  $[\text{Ru}(\eta^6\text{-C}_6\text{Me}_6)(\text{bpy})(\text{NCCH}_3)]^{2+}$ , both the singly (probably  $n = 0$ ) and doubly ( $n = 0$ ) reduced species contribute to this electrochemical potential. The following estimation of acidities and bond dissociation free energies (BDFEs) of both hydride complexes depends on these assignments.

**The Acidity of [Ru(tpy)(bpy)H]<sup>+</sup> in Acetonitrile.** The acetonitrile data may be used to obtain thermodynamic estimates for heterolytic cleavage of [Ru(tpy)(bpy)H]<sup>+</sup> to yield H<sup>+</sup> and homolytic cleavage to yield an H atom.<sup>16</sup> To estimate the pK<sub>a</sub>, we use Scheme 3.

From the free-energy change we then estimate pK<sub>a</sub> of 32 ± 3 for [Ru(tpy)(bpy)H]<sup>+</sup> to be compared with the limits >23.3 and ~32.9 established by direct observations on the deprotonation, which should refer to [Ru(tpy)(bpy)]<sup>0</sup>, and then 35.2 and 42.6 obtained from DFT calculations, which refer to the reaction producing [Ru(tpy)(bpy)]<sup>0</sup> and [Ru(tpy)(bpy)(NCCH<sub>3</sub>)]<sup>0</sup>, respectively. The comparison shows that pK<sub>a</sub> of 32 referring to [Ru(tpy)(bpy)(NCCH<sub>3</sub>)]<sup>0</sup> is close to pK<sub>a</sub> referring to [Ru(tpy)(bpy)]<sup>0</sup>. This discrepancy implies that the free energy change upon loss of acetonitrile ligand is small.

**BDFEs in Acetonitrile.** Values for ΔG<sub>H<sup>•</sup></sub><sup>o</sup>, the free energy of bond homolysis, are obtained from the cycle given in Scheme 4.

#### Scheme 4. BDFE Estimation in Acetonitrile<sup>a</sup>

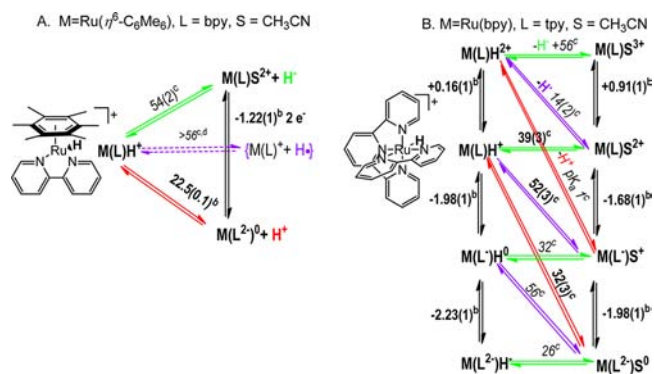
| Reaction   | ΔG <sup>o</sup> , kcal/mol   |
|--|--|
| MH <sup>+</sup> + CH <sub>3</sub> CN → [M(NCCH <sub>3</sub> ) <sub>n</sub> ] <sup>+</sup> + H <sup>+</sup>               | 1.364 pK <sub>a</sub> (M-H) = ΔG <sub>H<sup>•</sup></sub> <sup>o</sup>                               |
| H <sup>+</sup> + e <sup>-</sup> → H <sup>•</sup>   | 53.6 vs Fc <sup>+</sup> /Fc <sup>16</sup>  |
| [M(NCCH <sub>3</sub> ) <sub>n</sub> ] <sup>0</sup> → [M(NCCH <sub>3</sub> ) <sub>n</sub> ] <sup>+</sup> + e <sup>-</sup> | +23.06 E <sup>o</sup> (+/0)  |
| MH <sup>+</sup> + CH <sub>3</sub> CN → [M(NCCH <sub>3</sub> ) <sub>n</sub> ] <sup>+</sup> + H <sup>•</sup>               | ΔG <sub>H<sup>•</sup></sub> <sup>o</sup> = 1.364 pK <sub>a</sub> + 23.06 E <sup>o</sup> (+/0) + 53.6 |

<sup>a</sup>“M” denotes either Ru(η<sup>6</sup>-C<sub>6</sub>Me<sub>6</sub>)(bpy) for n = 0 or Ru(tpy)(bpy) for n = 1.

The ΔG<sub>H<sup>•</sup></sub><sup>o</sup> values ≥56 and 52 kcal/mol are obtained for [Ru(η<sup>6</sup>-C<sub>6</sub>Me<sub>6</sub>)(bpy)H]<sup>+</sup> and [Ru(tpy)(bpy)H]<sup>+</sup>, respectively. Note that for [Ru(η<sup>6</sup>-C<sub>6</sub>Me<sub>6</sub>)(bpy)]<sup>0</sup>, E<sup>o</sup>(+/0) may be less negative than the value used, since this complex undergoes two-electron reduction and coincidentally, for [Ru(η<sup>6</sup>-C<sub>6</sub>Me<sub>6</sub>)(bpy)(NCCH<sub>3</sub>)]<sup>2+</sup>, E<sup>o</sup>(2+/+) may also be more negative than the E<sup>o</sup>(2+/0) value. Consequently, the value calculated for [Ru(η<sup>6</sup>-C<sub>6</sub>Me<sub>6</sub>)(bpy)H]<sup>+</sup> is regarded as a lower limit and, however, probably not far from 56 kcal/mol because a purging of the hydride complex in acetonitrile (0.1 mM) with 2% oxygen gas balanced with Ar at 273 K in the dark caused loss of the MLCT band in the UV–vis spectrum on the time scale of 1 s, whereas [Ru(tpy)(bpy)(NCCH<sub>3</sub>)]<sup>+</sup> did not show such reactivity at all on this time scale (BDFE for •OO–H has been estimated as ~58 kcal/mol<sup>80</sup> in dimethyl sulfoxide, DMSO). Furthermore, these likely differ from commonly reported BDFEs, e.g., for R–H = R<sup>•</sup> + H<sup>•</sup>, because the reference state is the six-coordinate, i.e., [Ru(tpy)(bpy)(NCCH<sub>3</sub>)]<sup>+</sup>, not the five-coordinate species, i.e., [Ru(tpy)(bpy)]<sup>+</sup>, obtained from H-atom abstraction. One would expect the conventional BDFE referring to [Ru(tpy)(bpy)]<sup>+</sup> to be ca. 56 kcal/mol assuming that the difference from the BDFE of the six-coordinate species is the same as the difference between 64.3 and 59.6 kcal/mol obtained from the DFT calculations for producing the five- and six-coordinate species, respectively.

Including the acidities and BDFEs described just above, the results of our thermodynamic studies of [Ru(η<sup>6</sup>-C<sub>6</sub>Me<sub>6</sub>)(bpy)H]<sup>+</sup> and [Ru(tpy)(bpy)H]<sup>+</sup> are summarized in Scheme 5, and detailed calculations for [Ru(tpy)(bpy)H]<sup>+</sup> are given in Scheme S1 of the Supporting Information. Here we have adopted a notation that allows us to indicate that electrons added to the Ru(II) complexes enter a π\* orbital of bpy in [Ru(η<sup>6</sup>-C<sub>6</sub>Me<sub>6</sub>)(bpy)H]<sup>+</sup> and a π\* orbital of tpy in [Ru(tpy)(bpy)H]<sup>+</sup>, with the metal center essentially preserving its oxidation state as a

#### Scheme 5. Hydricities, BDFEs, and Acidities<sup>a</sup>



<sup>a</sup>Values to the left or right of vertical lines are reduction potentials vs Fc<sup>+</sup>/Fc in CH<sub>3</sub>CN. Values above horizontal or diagonal lines are free energy changes in kcal/mol except for those above red lines, which are pK<sub>a</sub> values in CH<sub>3</sub>CN. <sup>b</sup>From direct measurement of electrochemical potentials or chemical equilibria. <sup>c</sup>Obtained from thermochemical cycles; see the text and Scheme S1, Supporting Information. <sup>d</sup>Lower limit; see the text.

six-coordinate Ru(II) center. As discussed above, we are more confident of this description for the Ru(tpy)(bpy) series. Thus, in M(L)H<sup>+</sup> = [Ru(tpy)(bpy)H]<sup>+</sup>, M denotes the Ru<sup>II</sup>(bpy) fragment and L is the tpy ligand. The exception is the oxidized hydride complex M(L)H<sup>2+</sup>, which is [Ru<sup>III</sup>(tpy)(bpy)H]<sup>2+</sup>, but the reduced forms all contain Ru(II), i.e., [Ru<sup>II</sup>(tpy<sup>-</sup>)(bpy)H]<sup>0</sup> = M(L<sup>-</sup>)H<sup>0</sup>, [Ru<sup>II</sup>(tpy<sup>2-</sup>)(bpy)H]<sup>-</sup> = M(L<sup>2-</sup>)H<sup>-</sup>. The notation is analogous to that of the acetonitrile (S) complexes M(L<sup>-</sup>)S<sup>+</sup>, etc.

Several trends may be noted in the more extensive data set for [Ru(tpy)(bpy)H]<sup>+</sup>. Hydride donor ability increases as electrons are added: starting with [Ru(tpy)(bpy)H]<sup>2+</sup> and adding one-electron steps the hydricities increase from +56 to +39, +32, and +26 kcal/mol for [Ru(tpy<sup>2-</sup>)(bpy)H]<sup>-</sup>. BDFEs are similar for [Ru(tpy)(bpy)H]<sup>0</sup> and [Ru(tpy)(bpy)H]<sup>+</sup> (56 kcal/mol), but quite small for [Ru(tpy)(bpy)H]<sup>2+</sup> (14 kcal/mol). Acidity increases greatly on oxidation of [Ru(tpy)(bpy)H]<sup>+</sup> (pK<sub>a</sub> = 32) by one electron, pK<sub>a</sub>([Ru(tpy)(bpy)H]<sup>2+</sup>) = 1.

The implication of the ligand-centered electronic structural assignments is that protonation of [Ru(tpy)(bpy)(NCCH<sub>3</sub>)<sub>n</sub>]<sup>0</sup> (and probably [Ru(η<sup>6</sup>-C<sub>6</sub>Me<sub>6</sub>)(bpy)]<sup>0</sup>) differs qualitatively from protonation of other transition-metal systems, for example, low-spin, square-planar d<sup>8</sup> complexes in which the electron pair to be protonated lies in the d<sub>z<sup>2</sup></sub> orbital, since the electrons to be protonated in [Ru(tpy)(bpy)(NCCH<sub>3</sub>)]<sup>0</sup> are delocalized over ligand π\* and metal levels. To better understand this process, we have calculated the electronic structures of [Ru(tpy)(bpy)(NCCH<sub>3</sub>)]<sup>0</sup>, [Ru(tpy)(bpy)]<sup>0</sup>, and [Ru(tpy)(bpy)]<sup>0</sup> + H<sup>+</sup> complex (simulated as [Ru(tpy)(bpy)H]<sup>+</sup> with a stretched Ru–H bond of 2 Å in order to simulate proton approach prior to proton transfer). As depicted in Figure 9 (see also Supporting Information, Figure S11), protonation could involve [Ru(tpy)(bpy)(NCCH<sub>3</sub>)]<sup>0</sup> or the (singlet) “five-coordinate” [Ru(tpy)(bpy)]<sup>0</sup>. Loss of CH<sub>3</sub>CN results in a localization of the excess electron pair in an orbital that is delocalized over the d<sub>xz</sub> of Ru and the lowest π\* orbital of tpy. A proton approaching the Ru along the z axis would have no interaction with this HOMO, but would interact with the doubly occupied d<sub>z<sup>2</sup></sub> orbital (HOMO – 1, Orb. 109) of the Ru. The resulting Ru–H σ bonding orbital is stabilized from HOMO – 1 to HOMO – 3 (Orb. 107 on the right of Figure 9). There is also a contribution to the Ru–H bond involving one lobe of the d<sub>xz</sub> orbital on Ru.

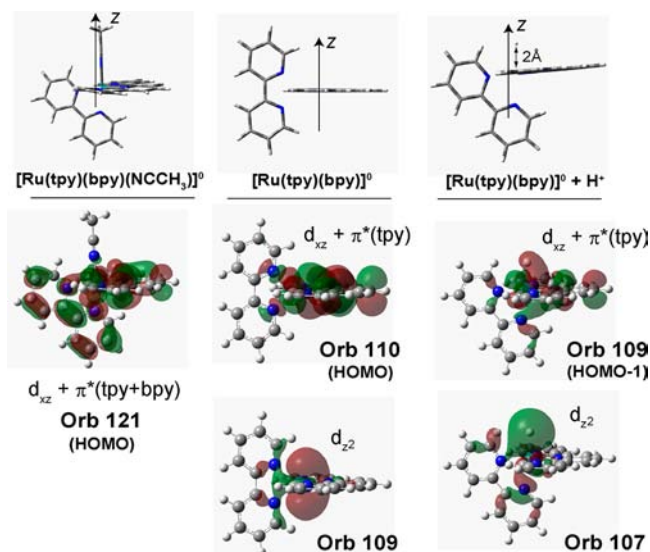


**Figure 9.** Selected valence DFT orbitals for (left to right)  $[\text{Ru}(\text{tpy})(\text{bpy})(\text{NCCH}_3)]^0$ ,  $[\text{Ru}(\text{tpy})(\text{bpy})]^0$ , and  $[\text{Ru}(\text{tpy})(\text{bpy})]^0 + \text{H}^+$  (simulated as  $[\text{Ru}(\text{tpy})(\text{bpy})\text{H}]^+$  with a stretched Ru–H bond of 2 Å). The blue arrow in the top panel of the stick diagrams defines the  $z$  axis; bpy lies in the  $xz$  plane. In  $[\text{Ru}(\text{tpy})(\text{bpy})(\text{NCCH}_3)]^{2+}$ , orbital 121 is  $d_{xy}$ , although one lobe of it “reaches around” to participate in a  $\pi^*$  orbital on the bpy; this symmetry breaking is allowed by the fact that the tpy is canted away from a symmetrical position.

With this complication in mind, we nonetheless consider comparisons with other metal hydrides regarding the contributions to the thermodynamics of hydricity, and the mechanisms of hydride ion transfer.

**Comparisons with Other Metal Hydride Complexes in Acetonitrile Solvent.** Several kinds of comparisons can now be made with other transition-metal hydrides. The  $\text{Ru}^{\text{II}}$  hydrides studied here exhibit hydricities within the range already defined by the extensive work of DuBois in acetonitrile.<sup>72</sup> The acidities of  $[\text{Ru}(\eta^6\text{-C}_6\text{Me}_6)(\text{bpy})\text{H}]^+$  (22.5) and  $[\text{Ru}(\text{tpy})(\text{bpy})\text{H}]^+$  (32) in acetonitrile bracket that reported recently by Norton’s group for  $\text{CpRu}(\text{CO})_2\text{H}$  (28.3).<sup>11</sup> That of  $[\text{Ru}(\text{tpy})(\text{bpy})\text{H}]^+$  (32) is similar to that of Bullock’s  $\text{W}(\text{CO})_2(\text{Mes})\text{H}$ ,<sup>17</sup> which was deprotonated with the same proazaphosphatane base as used here.

For a more quantitative comparison, the thermodynamic relationship shown in eq 17 (derived from another thermodynamic cycle; Supporting Information, Scheme S2)

$$\Delta G_{\text{H}^-}^\circ = \Delta G_{\text{H}^\bullet}^\circ - F[E^\circ(\text{H}^\bullet/\text{H}^-) - E^\circ(\text{M}^+/\text{M}^0)] \quad (17)$$

can be used as a measure. For example, DuBois has already noted the correlation of hydricity with the  $d^8/d^9 \text{Ni}(\text{II})/(\text{I})$  potential.<sup>81</sup> Figure 10 shows the correlation between our results and hydricity values reported by DuBois,<sup>12,16,81–86</sup> Bruno,<sup>87</sup> Savéant,<sup>88</sup> and Moiroux<sup>89</sup> for various kinds of hydride donors [three sets of monohydride complexes containing Ni(II), Pd(II), and Re(I) for which the first reduction potentials are available and which consist of more than two complexes in each set;  $\text{NAD}^+$  model compounds; triarylcarboniums; and  $\text{H}_2$ ] vs the second term on the right-hand of eq 17 (see also Supporting Information, Table S4). Lines of unit slope are imposed on the points of each class plotted; their zero intercepts correspond to a BDFE for each class at zero electrochemical driving force.

According to this classification,  $[\text{Ru}(\eta^6\text{-C}_6\text{Me}_6)(\text{bpy})\text{H}]^+$  is in the same class as Ni(II) and Pd(II) mono hydride complexes

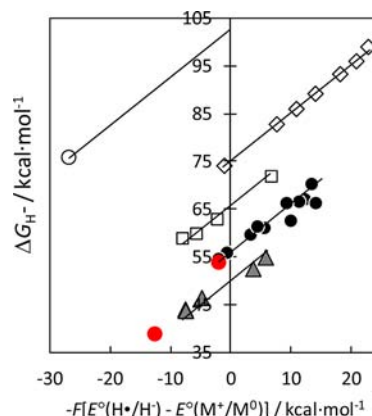


**Figure 10.** Correlations between hydricities for various kinds of hydride donor vs the difference between the second reduction potential for the conjugate hydride acceptor and the reduction potential of the  $\text{H}^\bullet/\text{H}^-$  couple (black circle, monohydride metal complexes; red circle, the complexes studied here; open square,  $\text{NAD}^+$  models; open diamond, triarylcarboniums; gray triangle, Re(I) formyl complexes; and open circle,  $\text{H}_2$ ) in acetonitrile. Slopes of lines are set to unity. For  $[\text{Ru}(\eta^6\text{-C}_6\text{Me}_6)(\text{bpy})\text{H}]^+$ ,  $E^\circ(2+/0)$  of  $[\text{Ru}(\eta^6\text{-C}_6\text{Me}_6)(\text{bpy})(\text{NCCH}_3)_{1/0}]^{2+/0}$  is used as a positive limit of  $[\text{Ru}(\eta^6\text{-C}_6\text{Me}_6)(\text{bpy})(\text{NCCH}_3)]^{2+/+}$ .

having bis(diphosphino) ligands, or possibly  $\text{NAD}^+$  models since the BDFE of  $[\text{Ru}(\eta^6\text{-C}_6\text{Me}_6)(\text{bpy})\text{H}]^+$  and the first redox potential of  $[\text{Ru}(\eta^6\text{-C}_6\text{Me}_6)(\text{bpy})(\text{NCCH}_3)]^{2+}$  are estimated values as described above. Whereas  $[\text{Ru}(\text{tpy})(\text{bpy})\text{H}]^+$  is in the same class as Re(I) formyl complexes. This difference is caused by properties of  $\eta^6\text{-C}_6\text{Me}_6$  and tpy ligands, and can be divided into two factors: their effect on the redox potential as the major one; and the stability of the acetonitrile ligand in the singly reduced species as a possible minor one.

**Contributions of Solvents to Hydricities.** Previously, we estimated the hydricities of  $[\text{Ru}(\eta^6\text{-C}_6\text{Me}_6)(\text{bpy})\text{H}]^+$  and  $[\text{Ru}(\text{tpy})(\text{bpy})\text{H}]^+$  in water by equilibrating them with carbon dioxide and formate anion. To estimate their acidities in water, we use the hydricity values for water and the estimated  $E^\circ(2+/0)$  values quoted in Table 1 and Figures 1 and 2. The values and cycles used are shown below in Scheme 6, where we assume  $n = 0$  for  $[\text{Ru}(\eta^6\text{-C}_6\text{Me}_6)(\text{bpy})(\text{OH}_2)_n]^0$  and  $n = 1$  for  $[\text{Ru}(\text{tpy})(\text{bpy})(\text{OH}_2)_n]^0$ .

The  $\text{pK}_a$  value for  $[\text{Ru}(\text{tpy})(\text{bpy})\text{H}]^+$  is thus estimated as  $\geq 24$  in water, consistent with its failure to deprotonate at pH 12–13.<sup>90</sup> The value calculated for  $[\text{Ru}(\eta^6\text{-C}_6\text{Me}_6)(\text{bpy})\text{H}]^+$ ,  $\geq 6$ , is not consistent with the other observations: For  $[\text{Ru}(\eta^6\text{-C}_6\text{Me}_6)(\text{bpy})\text{H}]^+$  we could not observe the deprotonated species in pH 9 borate buffer, but instead found formation of  $[\text{Ru}(\eta^6\text{-C}_6\text{Me}_6)(\text{bpy})(\text{OH})]^+$ .<sup>79</sup> This may indicate that deprotonation of  $[\text{Ru}(\eta^6\text{-C}_6\text{Me}_6)(\text{bpy})\text{H}]^+$  results in reduction of  $[\text{Ru}(\eta^6\text{-C}_6\text{Me}_6)(\text{bpy})\text{H}]^+$  to  $\text{H}_2$  with formation of  $[\text{Ru}(\eta^6\text{-C}_6\text{Me}_6)(\text{bpy})(\text{OH})]^+$ . Further investigation is needed to clarify this chemistry.

What determines different hydricities in water and acetonitrile? The thermodynamics of transfer of ions and molecules from water to organic solvents (with use of an extra thermodynamic assumption) have been extensively studied.<sup>91,92</sup> Solvents of high donor number stabilize cations,<sup>93</sup> while solvents of high acceptor number stabilize anions.<sup>94</sup> An estimation of the stabilization energy for hydride anion is still a challenging problem. One of the ways is linear extrapolation/interpolation of the value from those of  $\text{I}^-$ ,  $\text{Br}^-$ , and  $\text{F}^-$  series based on the Born electrostatic model for solvation.<sup>95</sup> Accordingly, the hydride ion

Scheme 6. Acidity Estimation in Water<sup>a</sup>

| Reaction for M(L) <sup>z+</sup>   |   | Ru( $\eta^6$ -C <sub>6</sub> Me <sub>6</sub> )(bpy) | Ru(tpy)(bpy)   |
|---|---|---|--|
| MH <sup>+</sup> + H <sub>2</sub> O<br>→ M(OH <sub>2</sub> ) <sup>2+</sup> + H <sup>-</sup>                | ( $\Delta G_{\text{tr}}^{\circ}$ , kcal/mol)  | 31 <sup>9</sup>                                     | 22 <sup>9</sup>  |
| M(OH <sub>2</sub> ) <sup>2+</sup> + 2e <sup>-</sup><br>→ [M(OH <sub>2</sub> ) <sub>n</sub> ] <sup>0</sup> | (-nFE <sup>o</sup> vs NHE)  | ≥26<br>(E <sup>o</sup> (2+/0) ≤ -0.57 V)            | ≥59<br>E <sup>o</sup> (2+/+) ≤ -1.19 V<br>E <sup>o</sup> (+/0) ≤ -1.38 V |
| H <sup>-</sup> → H <sup>+</sup> + 2e <sup>-</sup>   | ( $\Delta G^{\circ}$ , kcal/mol)  | -48.7 vs NHE <sup>13</sup>                          | -48.7 vs NHE <sup>13</sup>   |
| MH <sup>+</sup> + H <sub>2</sub> O<br>→ [M(OH <sub>2</sub> ) <sub>n</sub> ] <sup>0</sup> + H <sup>+</sup> | $\left[ \begin{array}{l} \Delta G_{\text{tr}}^{\circ}, \text{ kcal/mol} \\ (\text{p}K_{\text{a}}(\text{MH}^+)) \end{array} \right]$ | ≥8<br>(≥6)  | ≥32<br>(≥24)   |

<sup>a</sup>"M" denotes either Ru( $\eta^6$ -C<sub>6</sub>Me<sub>6</sub>)(bpy) for n = 0 or Ru(tpy)(bpy) for n = 1.

Table 4. Thermodynamics in Acetonitrile and Water (1 M standard states, 298 K)<sup>a</sup>

| reaction for M(L) <sup>z+</sup>   | solvent                                | [Ru( $\eta^6$ -C <sub>6</sub> Me <sub>6</sub> )(bpy)H] <sup>+</sup> |  | [Ru(tpy)(bpy)H] <sup>+</sup>  |  |
|---|--|---|--|---|--|
|   |  | parameter   | $\Delta G^{\circ}$ , kcal/mol                          | parameter   | $\Delta G^{\circ}$ , kcal/mol                          |
| H <sup>+</sup> + 2e <sup>-</sup> → H <sup>-</sup><br>(vs Fc <sup>+</sup> /Fc based on +0.528 V vs NHE) <sup>15</sup><br>(vs NHE)                            | CH <sub>3</sub> CN<br>H <sub>2</sub> O |   | 79.6 <sup>12</sup><br>48.7 <sup>13</sup>               |   | 79.6 <sup>12</sup><br>48.7 <sup>13</sup>               |
| M(S) <sup>2+</sup> + 2e <sup>-</sup> → M(S) <sub>n</sub> <sup>0</sup><br>E <sup>o</sup> (2+/0), V vs Fc <sup>+</sup> /Fc<br>E <sup>o</sup> (2+/0), V vs NHE | CH <sub>3</sub> CN<br>H <sub>2</sub> O | E <sup>o</sup> (2+/0):<br>-1.22<br>≤ -0.57                          | 56<br>≥26  | E <sup>o</sup> (2+/0):<br>-1.83 <sup>b</sup><br>(≤ -1.3) <sup>b</sup> | 84<br>(≥59)  |
| MH <sup>+</sup> + S → M(S) <sup>2+</sup> + H <sup>-</sup>   | CH <sub>3</sub> CN<br>H <sub>2</sub> O |   | ( $\Delta G_{\text{tr}}^{\circ}$ )<br>54 ± 2<br>31 ± 2 |   | ( $\Delta G_{\text{tr}}^{\circ}$ )<br>39 ± 3<br>22 ± 2 |
| MH <sup>+</sup> + S → M(S) <sub>n</sub> <sup>0</sup> + H <sup>+</sup>   | CH <sub>3</sub> CN<br>H <sub>2</sub> O | pK <sub>a</sub> :<br>22.5 ± 0.1<br>≥6.4                             | 30.7 ± 0.1<br>≥8.8                                     | pK <sub>a</sub> :<br>32 ± 3<br>≥24                                    | 44 ± 3<br>≥32  |
| M(OH <sub>2</sub> ) <sup>2+</sup> + CH <sub>3</sub> CN → M(NCCH <sub>3</sub> ) <sup>2+</sup> + H <sub>2</sub> O   | CH <sub>3</sub> CN/H <sub>2</sub> O    |   |  | K: 13 ± 4   | -1.5 ± 0.2   |

<sup>a</sup>"M" denotes either Ru( $\eta^6$ -C<sub>6</sub>Me<sub>6</sub>)(bpy) of n = 0 or Ru(tpy)(bpy) in n = 1. <sup>b</sup>Average of potentials for first and second reductions, which are actually ligand centered.

is stabilized by ca. 16–22 kcal/mol in water compared to acetonitrile,<sup>90,93</sup>  $\Delta G_{\text{tr}}^{\circ}(\text{H}^-)_{\text{w} \rightarrow \text{s}}$ , to be compared with the observed shifts in hydricity for [Ru( $\eta^6$ -C<sub>6</sub>Me<sub>6</sub>)(bpy)H]<sup>+</sup> and [Ru(tpy)(bpy)H]<sup>+</sup> of 23 ± 2 and 17 ± 3 kcal/mol, respectively, for transfer from acetonitrile to water. The thermodynamics for the present systems are considered in Table 4. The electrochemical potentials [E<sup>o</sup>(2+/0)] do not shift greatly with solvent (the apparent difference in Table 4 is mainly due to use of different reference electrodes in the two solvents. See also Table 1), but the acidity of [Ru(tpy)(bpy)H]<sup>+</sup> increases in water by ~8 pK<sub>a</sub> units. Water increases the hydride donor power of [Ru(tpy)(bpy)H]<sup>+</sup> by 17 ± 2 kcal/mol ( $\Delta_{\text{tr}}(\Delta G_{\text{tr}}^{\circ})_{\text{w} \rightarrow \text{s}}$ ), despite the fact that acetonitrile as a ligand stabilizes Ru(II) 1.5 kcal/mol more than water ( $\Delta G_{\text{ex}}^{\circ}$ ). Equation 18 shows a thermodynamic relationship among these quantities, where  $\Delta G_{\text{tr}}^{\circ}(X)_{\text{w} \rightarrow \text{s}}$  is the free-energy change on transfer of an ion,<sup>91</sup> X, from water to acetonitrile.

$$\begin{aligned} \Delta_{\text{tr}}(\Delta G_{\text{tr}}^{\circ})_{\text{w} \rightarrow \text{s}} &= \Delta G_{\text{tr}}^{\circ}(\text{H}^-)_{\text{w} \rightarrow \text{s}} + \Delta G_{\text{tr}}^{\circ}(\text{M}^{2+})_{\text{w} \rightarrow \text{s}} \\ &+ \Delta G_{\text{ex}}^{\circ} - \Delta G_{\text{tr}}^{\circ}(\text{MH}^+)_{\text{w} \rightarrow \text{s}} \\ &= 17 \text{ kcal/mol, for } [\text{Ru}(\text{tpy})(\text{bpy})\text{H}]^+ \end{aligned} \quad (18)$$

Thus the behavior of the present systems indicates that the increased donor power of these hydride complexes in water is due to hydrogen-bonding stabilization of free hydride ion, with only a small or negligible contribution from the differential

stabilization of +2-charged solvent complex conjugate acceptor and the second and fourth terms in the right-hand seem to cancel.

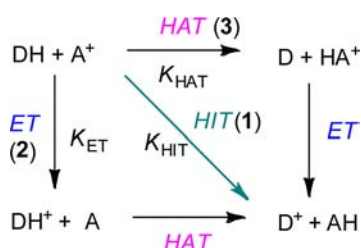
We should also note that the differential stabilization is expected to take a small value for small anion molecules because small anions tend<sup>91,92</sup> to take positive values of  $\Delta G_{\text{tr}}^{\circ}(X)_{\text{w} \rightarrow \text{s}}$ , e.g., [HCO<sub>2</sub>]<sup>-</sup> for which the smaller change on the hydricity from water (35 kcal/mol<sup>9</sup>) to acetonitrile (47 ± 4<sup>3,86</sup> or 43 ± 2 kcal/mol<sup>74</sup>) was observed (eq 18).

$$\begin{aligned} \Delta_{\text{tr}}(\Delta G_{\text{tr}}^{\circ})_{\text{w} \rightarrow \text{s}} &= \Delta G_{\text{tr}}^{\circ}(\text{H}^-)_{\text{w} \rightarrow \text{s}} + \Delta G_{\text{tr}}^{\circ}(\text{CO}_2)_{\text{w} \rightarrow \text{s}} \\ &- \Delta G_{\text{tr}}^{\circ}(\text{HCO}_2^-)_{\text{w} \rightarrow \text{s}} \\ &= 12 \text{ or } 8 \text{ kcal/mol} \end{aligned} \quad (18a)$$

**Mechanisms of Hydride Transfer Reactions.** Hydride transfer reactions may occur in single or multiple steps as indicated in Scheme 7, in which DH and A<sup>+</sup> are hydride donor and acceptor, respectively, and electron transfers are vertical and H-atom transfers are horizontal.

The diagonal line HIT (1) is the direct pathway characterized by the equilibrium constant K<sub>H<sup>-</sup></sub>. Pathway 2, ET, is initiated by electron transfer from DH to A<sup>+</sup>. For metal hydrides, the low intrinsic barrier to H-atom transfer leads to the additional consideration of initial H-atom transfer, followed by electron transfer (top horizontal, pathway 3). Metal hydrides, hydride acceptors, and thermodynamic and kinetic parameters for hydride acceptors are listed in Supporting Information, Table

## Scheme 7. Hydride Transfer Paths



S1; the abbreviations are given in Chart 1. Electron-transfer and H-atom transfer alternatives are treated in the Supporting Information (Tables S2 and S3). Table 5 summarizes the results of the analysis of the energetics.

Net hydride ion transfer may occur via a two-step mechanism initiated either by an electron or H-atom transfer (Scheme 7). For the reaction pairs given in Table 5 the equilibrium constants for outer-sphere electron transfer are  $<10^{-23}$  (Table S2 in Supporting Information), so that the maximum second-order rate constant possible via this pathway is  $<10^{-13} \text{ M}^{-1} \text{ s}^{-1}$  assuming a rate constant of  $k_{\text{max}} = 10^{10} \text{ M}^{-1} \text{ s}^{-1}$  for the subsequent H-atom transfer. Similarly, for the three entries given, initial H-atom transfer is sufficiently endergonic that hydride ion transfer is clearly the prevalent pathway.

Previously, hydride transfer from  $[\text{Ru}(\text{tpy})(\text{bpy})\text{H}]^+$  to acceptors  $\text{BNA}^+$  (entry 1)<sup>96</sup> and  $\text{CO}_2$  (entry 3<sup>77,97</sup>) were found to involve “Ru–A–H” species as primary products. There is evidence that the cationic imidazolium and pyridinium acceptors (entries 4–6) react in the same way with  $[\text{Ru}(\text{tpy})(\text{bpy})\text{H}]^+$ . By contrast, reaction with  $[\text{Ru}(\eta^6\text{-C}_6\text{Me}_6)(\text{bpy})(\text{NCCH}_3)]^{2+}$  yields a hydride-bridged intermediate “Ru–H–A” species (entry 2). Thus, none of these reactions occur by a so-called “outer-sphere” mode. However, despite the formation of the “inner-sphere” product in which the reduced acceptor is bound to Ru(II) either through a heteroatom or  $\eta^2$  to a C=C bond, there is no evidence for binding of the hydride acceptor to the donor prior to the rate-determining hydride transfer step. As noted by Ellis et al. for isoelectronic W compounds yielding bridged W–O(H)C–Re primary products:<sup>72</sup> “These reactions all appear to occur by a common pathway of hydride transfer followed by rearrangement to form an intermediate with an M–O bond and then slow solvolysis of the M–O bond.”

**Driving Force Dependence.** An additional intriguing aspect of the hydride transfer data obtained for  $[\text{Ru}(\text{tpy})(\text{bpy})\text{H}]^+$  is the linear dependence of activation free energy on acceptor hydricity over a very large hydricity range (Supporting Information, Figure S13, left). This parallels observations of Kreevov for hydride transfer to pyridinium acceptors from

NADH-type donors.<sup>98</sup> In the light of the comparison of intrinsic energy potential of the two hydride donors at zero driving force gauged by the intercepts of  $-7.5$  for the complex and  $-5.5$  for NADH-type donors, respectively, on the linear dependences (smaller intercept means here larger potential),  $[\text{Ru}(\text{tpy})(\text{bpy})\text{H}]^+$  is a somewhat slower hydride donor to pyridinium hydride acceptors, which is consistent with the observation that the self-exchange reaction of  $[\text{Ru}(\text{tpy})(\text{bpy})\text{H}]^+$  with  $[\text{Ru}(\text{tpy})(\text{bpy})(\text{NCCH}_3)]^{2+}$  is  $<3 \times 10^{-6} \text{ M}^{-1} \text{ s}^{-1}$ . We also note that the slope of the linear dependence is 0.4 (left in Supporting Information, Figure S13) and that slopes of around 0.5 are commonly observed for hydride transfer between purely organic reactants.<sup>99,100</sup> However, these conclusions are tentative and merit more systematic investigation.

## CONCLUDING REMARKS

At the outset our purposes were to determine hydricities in acetonitrile that could be compared with values for other hydride donor systems, including organic and transition-metal complexes. We also wanted to determine rate constants for hydride transfer reactions and relate them to reaction thermodynamics. Rather remarkably,  $[\text{Ru}(\eta^6\text{-C}_6\text{Me}_6)(\text{bpy})]^0$  and  $[\text{Ru}(\text{tpy})(\text{bpy})]^0$ , which are the conjugate bases of  $[\text{Ru}(\eta^6\text{-C}_6\text{Me}_6)(\text{bpy})\text{H}]^+$  and  $[\text{Ru}(\text{tpy})(\text{bpy})\text{H}]^+$ , are Ru(II) complexes of  $(\text{bpy}^{2-})$  and  $(\text{tpy}^{2-})$ , respectively, on which two electrons are localized. We have shown that  $[\text{Ru}(\eta^6\text{-C}_6\text{Me}_6)(\text{bpy})\text{H}]^+$  and  $[\text{Ru}(\text{tpy})(\text{bpy})\text{H}]^+$  are better hydride donors in water than in acetonitrile by  $\sim 20 \text{ kcal/mol}$ , with the bulk (if not all) of that difference being due to stabilization of the hydride ion in water, i.e., the protic, high acceptor number solvent. Indeed, water promotes stronger hydride donation, but also appears to narrow the observed hydricity range. The hydride transfer reactions are intrinsically slow in acetonitrile and always involve formation of a product complex in which the reduced hydride acceptor is bound to Ru(II) either through a heteroatom or  $\eta^2$  to a C=C bond. Similarly, reactions of these hydride complexes with potential transition-metal acceptors yield hydride-bridged, bimetallic products.

## ASSOCIATED CONTENT

### Supporting Information

Additional electrochemical, electronic spectral, and NMR data; valence orbitals; coordinates; and complete ref 45. This material is available free of charge via the Internet at <http://pubs.acs.org/>.

## AUTHOR INFORMATION

### Corresponding Author

ccreutz@bnl.gov

Table 5. Kinetics and Thermodynamics of Hydride Transfer Reactions of  $[\text{Ru}(\text{tpy})(\text{bpy})\text{H}]^+$  in Acetonitrile at 298 K<sup>a</sup>

| entry | acceptor (A <sup>+</sup> )  | $k_b \text{ M}^{-1} \text{ s}^{-1}$ | step 1<br>$\log(K_{\text{HIT}})^b$ | step 2<br>$\log(K_{\text{ET}})$ | step 3<br>$\log(K_{\text{HAT}})$ |
|-------|---|-------------------------------------|------------------------------------|---------------------------------|----------------------------------|
| 1     | BNA <sup>+</sup>  | $1.7 \times 10^{3c}$                | 14.7                               | $<-27$                          | $<-21$                           |
| 2     | $[\text{Ru}(\eta^6\text{-C}_6\text{Me}_6)(\text{bpy})(\text{NCCH}_3)]^{2+}$ | $\geq 4 \times 10^{-1d}$            | 11                                 | $<-23$                          | $e$                              |
| 3     | CO <sub>2</sub>   | $1.8 \times 10^{-2.37}$             | 2.9                                | $e$                             | $e$                              |
| 4     | BMPy <sup>+</sup>   | $1.5 \times 10^{-2}$                | 2.9                                | $<-32$                          | $<-27$                           |
| 5     | BzIm <sup>+</sup>   | $6.5 \times 10^{-3}$                | $e$                                | $<-37$                          | $e$                              |
| 6     | DMPy <sup>+</sup>   | $1.6 \times 10^{-3f}$               | 1.5                                | $<-33$                          | $e$                              |
| 7     | $[\text{Ru}(\text{tpy})(\text{bpy}-d_8)(\text{NCCH}_3)]^{2+}$               | $<3 \times 10^{-6}$                 | 0                                  | -31                             | $e$                              |

<sup>a</sup>See the Supporting Information (Tables S1–S3) for details. <sup>b</sup>Calculated from the hydricities tabulated. See the text. <sup>c</sup> $k_{\text{solv}} = 3 \times 10^{-4} \text{ s}^{-1}$  at 300 K in DMF. <sup>d</sup> $k_{\text{solv}} = 7.5 \times 10^{-4} \text{ s}^{-1}$ . <sup>e</sup>Unknown. <sup>f</sup>A second-order rate constant of the reverse reaction ( $k_r$ ) is  $(9.2 \pm 3.2) \times 10^{-5} \text{ M}^{-1} \text{ s}^{-1}$ .

## Notes

The authors declare no competing financial interest.

## ACKNOWLEDGMENTS

This research was carried out at Brookhaven National Laboratory under contract DE-AC02-98CH10884 with the U.S. Department of Energy and supported by its Division of Chemical Sciences, Geosciences and Biosciences of the Office of Basic Energy Sciences. Y.M. acknowledges partial support (Nov 21, 2011–present) by the PRESTO project: “Chemical Conversion of Light Energy” of Japan Science and Technology Agency (JST). C.C. gratefully acknowledges the work of N. R. Abu-Rustum and P. J. Sabbatini, which made this contribution possible.

## REFERENCES

- (1) Wolf, J. F.; Staley, R. H.; Koppel, I.; Taagepera, M.; McIver, R. T.; Beauchamp, J. L.; Taft, R. W. *J. Am. Chem. Soc.* **1977**, *99*, 5417–5429.
- (2) Handoo, K. L.; Cheng, J. P.; Parker, V. D. *J. Am. Chem. Soc.* **1993**, *115*, 5067–5072.
- (3) DuBois, D. L.; Berning, D. E. *Appl. Organomet. Chem.* **2000**, *14*, 860–862.
- (4) Note this differs from the convention used by DuBois,<sup>3</sup> who originally considered only  $n = 0$  systems.
- (5) Balaraman, E.; Gunanathan, C.; Zhang, J.; Shimon, L. J. W.; Milstein, D. *Nat. Chem.* **2011**, *3*, 609–614.
- (6) Matsumura, K.; Arai, N.; Hori, K.; Saito, T.; Sayo, N.; Ohkuma, T. *J. Am. Chem. Soc.* **2011**, *133*, 10696–10699.
- (7) Guan, H. R.; Saddoughi, S. A.; Shaw, A. P.; Norton, J. R. *Organometallics* **2005**, *24*, 6358–6364.
- (8) *Basic Research Needs for Solar Energy Utilization, Report of the Basic Energy Sciences Workshop on Solar Energy Utilization, April 18–21, 2005*; Office of Science, U.S. DOE: Bethesda, MD, 2005.
- (9) Creutz, C.; Chou, M. H. *J. Am. Chem. Soc.* **2009**, *131*, 2794–2795.
- (10) Creutz, C.; Chou, M. H.; Hou, H.; Muckerman, J. T. *Inorg. Chem.* **2010**, *49*, 9809–9822.
- (11) Estes, D. P.; Vannucci, A. K.; Hall, A. R.; Lichtenberger, D. L.; Norton, J. R. *Organometallics* **2011**, *30*, 3444–3447.
- (12) Berning, D. E.; Noll, B. C.; DuBois, D. L. *J. Am. Chem. Soc.* **1999**, *121*, 11432–11447.
- (13) Wayner, D. D. M.; Parker, V. D. *Acc. Chem. Res.* **1993**, *26*, 287–294.
- (14) Pavlishchuk, V. V.; Addison, A. W. *Inorg. Chim. Acta* **2000**, *298*, 97–102.
- (15) Although +0.630 V vs NHE is more widely accepted value for the  $\text{Fc}^+/\text{Fc}$  couple in acetonitrile,<sup>14</sup> we adopt the value (+0.528 V vs NHE originally reported in Parker, V. D., et al. *J. Am. Chem. Soc.* **1991**, *113*, 7493.) for consistency with other values for hydricities ( $\Delta G_{\text{H}^-}^\circ$ ), BDFEs ( $\Delta G_{\text{H}^\bullet}^\circ$ ), and acidities ( $\Delta G_{\text{H}^+}^\circ$ ) in acetonitrile have been reported so far. This adaptation implies that values in acetonitrile reported in this study is smaller for  $\Delta G_{\text{H}^-}^\circ$  and  $\Delta G_{\text{H}^\bullet}^\circ$ ; and larger for  $\Delta G_{\text{H}^+}^\circ$  by 2.3 kcal/mol compared with those calculated based on +0.630 V. This difference is comparable to uncertainties of those values and, therefore, does not affect qualitative comparison between those values in acetonitrile and water.
- (16) Ellis, W. W.; Raebiger, J. W.; Curtis, C. J.; Bruno, J. W.; DuBois, D. L. *J. Am. Chem. Soc.* **2004**, *126*, 2738–2743.
- (17) Roberts, J. A. S.; Appel, A. M.; DuBois, D. L.; Bullock, R. M. *J. Am. Chem. Soc.* **2011**, *133*, 14604–14613.
- (18) Roberts, J. A. S.; DuBois, D. L.; Bullock, R. M. *Organometallics* **2011**, *30*, 4555–4563.
- (19) Wilson, A. D.; Miller, A. J. M.; DuBois, D. L.; Labinger, J. A.; Bercaw, J. E. *Inorg. Chem.* **2010**, *49*, 3918–3926.
- (20) Lay, P. A.; McAlpine, N. S.; Hupp, J. T.; Weaver, M. J.; Sargeson, A. M. *Inorg. Chem.* **1990**, *29*, 4322–4328.
- (21) Siegbahn, P. E. M.; Eisenstein, O.; Rheingold, A. L.; Koetzle, T. F. *Acc. Chem. Res.* **1996**, *29*, 348–354.
- (22) Kristjánssdóttir, S. S.; Norton, J. R. *J. Am. Chem. Soc.* **1991**, *113*, 4366–4367.
- (23) Kristjánssdóttir, S. S.; Norton, J. R. Acidity of hydrido transition metal complexes in solution. In *Transition Metal Hydrides*; Dedieu, A., Ed.; VCH: New York, 1992; Chapter 9, pp 309–359.
- (24) Moore, E. J.; Sullivan, J. M.; Norton, J. R. *J. Am. Chem. Soc.* **1986**, *108*, 2257–2263.
- (25) Edidin, R. T.; Sullivan, J. M.; Norton, J. R. *J. Am. Chem. Soc.* **1987**, *109*, 3945–3953.
- (26) Jordan, R. F.; Norton, J. R. *J. Am. Chem. Soc.* **1982**, *104*, 1255–1263.
- (27) Angelici, R. J. *Acc. Chem. Res.* **1995**, *28*, 51–60.
- (28) Zhu, X.-Q.; Zhang, M.-T.; Yu, A.; Wang, C.-H.; Cheng, J.-P. *J. Am. Chem. Soc.* **2008**, *130*, 2501–2516.
- (29) Zhu, X.-Q.; Cao, L.; Liu, Y.; Yang, Y.; Lu, J.-Y.; Wang, J.-S.; Cheng, J.-P. *Chem.—Eur. J.* **2003**, *9*, 3937–3945.
- (30) Zhu, X. Q.; Tan, Y.; Cao, C. T. *J. Phys. Chem. B* **2010**, *114*, 2058–2075.
- (31) Zhu, X. Q.; Liu, Q. Y.; Chen, Q.; Mei, L. R. *J. Org. Chem.* **2010**, *75*, 789–808.
- (32) Richter, D.; Tan, Y.; Antipova, A.; Zhu, X. Q.; Mayr, H. *Asian J. Chem.* **2009**, *4*, 1824–1829.
- (33) Sarker, N.; Bruno, J. W. *J. Am. Chem. Soc.* **1999**, *121*, 2174–2180.
- (34) Cheng, T. Y.; Bullock, R. M. *Organometallics* **2002**, *21*, 2325–2331.
- (35) Cheng, T.-Y.; Brunschwig, B. S.; Bullock, R. M. *J. Am. Chem. Soc.* **1998**, *120*, 13121–13137.
- (36) Armarego, W. L. F.; Chai, C. L. L. *Purification of Laboratory Chemicals*, 5th ed.; Elsevier: Oxford, U.K., 2003.
- (37) Konno, H.; Kobayashi, A.; Sakamoto, K.; Fagalde, F.; Katz, N. E.; Saitoh, H.; Ishitani, O. *Inorg. Chim. Acta* **2000**, *299*, 155–163.
- (38) Hecker, C. R.; Fanwick, P. E.; McMillin, D. R. *Inorg. Chem.* **1991**, *30*, 659–666.
- (39) Hersh, W. H. *Inorg. Chem.* **1990**, *28*, 713–722.
- (40) Seurat, A.; Lemoine, P.; Gross, M. *Electrochim. Acta* **1978**, *23*, 1219–1225.
- (41) Miedaner, A.; Dubois, D. L.; Curtis, C. J.; Haltiwanger, R. C. *Organometallics* **1993**, *12*, 299–303.
- (42) Gulliver, D. J.; Levason, W.; Smith, K. G. *J. Chem. Soc., Dalton Trans.* **1981**, 2153–2158.
- (43) Salzer, C. A.; Elliott, C. M.; Hendrickson, S. M. *Anal. Chem.* **1999**, *71*, 3677–3683.
- (44) Bennett, M. A.; Huang, T. N.; Matheson, T. W.; Smith, A. K. *Inorg. Synth.* **1982**, *21*, 74–78.
- (45) Frisch, M. J. *Gaussian 09, Revision B.01*, Gaussian, Inc.: Wallingford, CT, 2009.
- (46) Becke, A. D. *Phys. Rev. A* **1988**, *38*, 3098–3100.
- (47) Lee, C.; Yang, W.; Parr, R. G. *Phys. Rev. B* **1988**, *37*, 785–789.
- (48) Vosko, S. H.; Wilk, L.; Nusair, M. *Can. J. Phys.* **1980**, *58*, 1200–1211.
- (49) Becke, A. D. *J. Chem. Phys.* **1993**, *98*, 5648–5652.
- (50) Stephens, P. J.; Devlin, F. J.; Chabalowski, C. F.; Frisch, M. J. *J. Phys. Chem.* **1994**, *98*, 11623–11627.
- (51) Andrae, D.; Haeussermann, U.; Dolg, M.; Stoll, H. *Preuss. Theor. Chim. Acta* **1990**, *77*, 123–141.
- (52) Martin, J. M. L.; Sundermann, A. *J. Chem. Phys.* **2001**, *114*, 3408–3420.
- (53) Gordon, M. S. *Chem. Phys. Lett.* **1980**, *76*, 163–168.
- (54) Hariharan, P. C.; Pople, J. A. *Theor. Chem. Acta* **1973**, *28*, 213–222.
- (55) Hariharan, P. C.; Pople, J. A. *Mol. Phys.* **1974**, *27*, 209–214.
- (56) Ditchfield, R.; Hehre, W. J.; Pople, J. A. *J. Chem. Phys.* **1971**, *54*, 724.
- (57) Hehre, W. J.; Ditchfield, R.; Pople, J. A. *J. Chem. Phys.* **1972**, *56*, 2257–&.
- (58) Francl, M. M.; Pietro, W. J.; Hehre, W. J.; Binkley, J. S.; Gordon, M. S.; Defrees, D. J.; Pople, J. A. *J. Chem. Phys.* **1982**, *77*, 3654–3665.
- (59) Miertus, S.; Tomasi, J. *Chem. Phys.* **1982**, *65*, 239–245.

- (60) Miertus, S.; Scrocco, E.; Tomasi, J. *Chem. Phys.* **1981**, *55*, 117–129.
- (61) Pascual-Ahuir, J. L.; Silla, E.; L., T. *J. Comput. Chem.* **1994**, *15*, 1127–1138.
- (62) Kaim, W.; Reinhardt, R.; Sieger, M. *Inorg. Chem.* **1994**, *33*, 4453–4459.
- (63) Stepnicka, P.; Ludvik, J.; Canivet, J.; Suss-Fink, G. *Inorg. Chim. Acta* **2006**, *359*, 2369–2374.
- (64) Rasmussen, S. C.; Ronco, S. E.; Mlsna, D. A.; Billadeau, M. A.; Pennington, W. T.; Kolis, J. W.; Petersen, J. D. *Inorg. Chem.* **1995**, *34*, 821–829.
- (65) Smith, K. T.; Romming, C.; Tilset, M. *J. Am. Chem. Soc.* **1993**, *115*, 8681–8689.
- (66) Bianchini, C.; Peruzzini, M.; Ceccanti, A.; Laschi, F.; Zanello, P. *Inorg. Chim. Acta* **1997**, *259*, 61–70.
- (67) Berger, R. M.; McMillin, D. R. *Inorg. Chem.* **1988**, *27*, 4245–4249.
- (68) Chen, Z.; Chen, C.; Weinberg, D. R.; Kang, P.; Concepcion, J. J.; Harrison, D. P.; Brookhart, M. S.; Meyer, T. J. *Chem. Commun.* **2011**, *47*, 12607–12609.
- (69) Kolthoff, I. M.; Chantooni, M. K.; Bhowmik, S. *J. Am. Chem. Soc.* **1968**, *90*, 23–28.
- (70) Kisanga, P. B.; Verkade, J. G. *J. Org. Chem.* **2000**, *65*, 5431.
- (71) Zhu, X. Q.; Li, H. R.; Li, Q.; Ai, T.; Lu, J. Y.; Yang, Y.; Cheng, J. P. *Chem.—Eur. J.* **2003**, *9*, 871–880.
- (72) Ellis, W. W.; Ciancanelli, R.; Miller, S. M.; Raebiger, J. W.; DuBois, M. R.; DuBois, D. L. *J. Am. Chem. Soc.* **2003**, *125*, 12230–12236.
- (73) Shaw, A. P.; Ryland, B. L.; Franklin, M. J.; Norton, J. R.; Chen, J. Y. C.; Hall, M. L. *J. Org. Chem.* **2008**, *73*, 9668–9674 and refs therein.
- (74) Price, A. J.; Ciancanelli, R.; Noll, B. C.; Curtis, C. J.; DuBois, D. L.; DuBois, M. R. *Organometallics* **2002**, *21*, 4833–4839.
- (75) Matsubara, Y.; Kosaka, T.; Nagasawa, A.; Kobayashi, A.; Konno, H.; Sakamoto, K.; Ishitani, O.; Creutz, C. *Organometallics* **2012**, to be submitted.
- (76) Darensbourg, M. Y.; Slater, S. J. *J. Am. Chem. Soc.* **1981**, *103*, 5914–5915.
- (77) Jahncke, M.; Meister, G.; Rheinwald, G.; Stoeckli-Evans, H.; Süss-Fink, G. *Organometallics* **1997**, *16*, 1137–1143.
- (78) Fowe, E. P.; Therrien, B.; Suss-Fink, G.; Daul, C. *Inorg. Chem.* **2008**, *47*, 42–48.
- (79) Chou, M. H.; Creutz, C. Unpublished observations.
- (80) Warren, J. J.; Tronic, T. A.; Mayer, J. M. *Chem. Rev.* **2010**, *110*, 6961–7001.
- (81) Berning, D. E.; Miedaner, A.; Curtis, C. J.; Noll, B. C.; DuBois, M. C. R.; Dubois, D. L. *Organometallics* **2001**, *20*, 1832–1839.
- (82) Ciancanelli, R.; Noll, B. C.; DuBois, D. L.; DuBois, M. R. *J. Am. Chem. Soc.* **2002**, *124*, 2984–2992.
- (83) Raebiger, J. W.; Miedaner, A.; Curtis, C. J.; Miller, S. M.; Anderson, O. P.; DuBois, D. L. *J. Am. Chem. Soc.* **2004**, *126*, 5502–5514.
- (84) Ellis, W. W.; Miedaner, A.; Curtis, C. J.; Gibson, D. H.; DuBois, D. L. *J. Am. Chem. Soc.* **2002**, *124*, 1926–1932.
- (85) Curtis, C. J.; Miedaner, A.; Raebiger, J. W.; DuBois, D. L. *Organometallics* **2004**, *23*, 511–516.
- (86) Curtis, C. J.; Miedaner, A.; Ellis, W. W.; DuBois, D. L. *J. Am. Chem. Soc.* **2002**, *124*, 1918–1925.
- (87) Zhang, X. M.; Bruno, J. W.; Enyinnaya, E. *J. Org. Chem.* **1998**, *63*, 4671–4678.
- (88) Hapiot, P.; Moiroux, J.; Saveant, J. M. *J. Am. Chem. Soc.* **1990**, *112*, 1337–1343.
- (89) Anne, A.; Moiroux, J. *J. Org. Chem.* **1990**, *55*, 4608–4614.
- (90) Creutz, C.; Chou, M. H. *J. Am. Chem. Soc.* **2007**, *129*, 10108–10109.
- (91) Marcus, Y.; Kamlet, M. J.; Taft, R. W. *J. Phys. Chem.* **1988**, *92*, 3613–3622.
- (92) Fawcett, W. R. *Langmuir* **2008**, *24*, 9868–9875.
- (93) Creutz, C. **2012**, manuscript in preparation.
- (94) Gutmann, V. *Electrochim. Acta* **1976**, *21*, 661–670.
- (95) Kelly, C. A.; Rosseinsky, D. R. *Phys. Chem. Chem. Phys.* **2001**, *3*, 2086–2090.
- (96) Kobayashi, A.; Takatori, R.; Kikuchi, I.; Konno, H.; Sakamoto, K.; Ishitani, O. *Organometallics* **2001**, *20*, 3361–3363.
- (97) Sullivan, B. P.; Meyer, T. *J. Organometallics* **1986**, *5*, 1500–1502.
- (98) Kreevoy, M. M.; Ostovic, D.; Lee, I. S. H.; Binder, D. A.; King, G. W. *J. Am. Chem. Soc.* **1988**, *110*, 524–530.
- (99) Lee, I. S. H.; Chow, K. H.; Kreevoy, M. M. *J. Am. Chem. Soc.* **2002**, *124*, 7755–7761.
- (100) Kim, Y.; Truhlar, D. G.; Kreevoy, M. M. *J. Am. Chem. Soc.* **1991**, *113*, 7837–7847.

#### NOTE ADDED IN PROOF

Our structural assumptions and conclusions about the basicity of  $[\text{Ru}(\eta^6\text{-C}_6\text{Me}_6)(\text{bpy})]^0$  are supported by results reported recently by Jeong et al. See: Jeong, K.; Nakamori, H.; Imai, S.; Matsumoto, T.; Ogo, S.; Nakai, H. *Chem. Lett.* **2012**, *41*, 650–651.